NASA TECHNICAL MEMORANDUM

NASA TM X-3539

NASA TM X-3539

GROUND CLOUD EFFLUENT MEASUREMENTS DURING THE MAY 30, 1974, TITAN III LAUNCH AT THE AIR FORCE EASTERN TEST RANGE

Richard J. Bendura and Kenneth H. Crumbly

Langley Research Center
Hampton, Va. 23665

NATIONAL AERONAUTICS AND SPACE ADMINISTRATION · WASHINGTON, D. C. · SEPTEMBER 1977

1. Report No.	2. Government Accession No.	3. Recipient's Catalog No.
NASA TM X-3539		

4. Title and Subtitle	5. Report Date
GROUND CLOUD EFFLUENT MEASUREMENTS DURING THE MAY 30, 1974, TITAN III LAUNCH AT THE AIR FORCE EASTERN TEST RANGE	September 1977
	6. Performing Organization Code

7. Author(s)	8. Performing Organization Report No.
Richard J. Bendura and Kenneth H. Crumbly	L-11372
	10. Work Unit No. 989-15-20-01

9. Performing Organization Name and Address	11. Contract or Grant No.
NASA Langley Research Center Hampton, VA 23665	
	13. Type of Report and Period Covered
12. Sponsoring Agency Name and Address	Technical Memorandum
National Aeronautics and Space Administration Washington, DC 20546	14. Sponsoring Agency Code

15. Supplementary Notes

16. Abstract

Surface-level exhaust effluent measurements of HCl, CO, and particulates, ground-cloud behavior, and some comparisons with model predictions for the launch of a Titan III rocket are presented along with a limited amount of airborne sampling measurements of other cloud species (O_3, NO, NO_x). Values above background levels for these effluents were obtained at 20 of the 30 instrument sites; these values were lower than model predictions and did not exceed public health standards. Cloud rise rate, stabilization altitude, and volume are compared with results from previous launches.

17. Key Words (Suggested by Author(s))	18. Distribution Statement
Effluent sampling Rocket vehicle exhaust Titan III exhaust effluents	Unclassified - Unlimited Subject Category 45

19. Security Classif. (of this report)	20. Security Classif. (of this page)	21. No. of Pages	22. Price*
Unclassified	Unclassified	49	$4.00

* For sale by the National Technical Information Service, Springfield, Virginia 22161

GROUND CLOUD EFFLUENT MEASUREMENTS DURING THE MAY 30, 1974, TITAN III LAUNCH AT THE AIR FORCE EASTERN TEST RANGE

Richard J. Bendura and Kenneth H. Crumbly
Langley Research Center

SUMMARY

Surface measurements of HCl, CO, and particulates from the exhaust effluent, ground-cloud behavior, and some comparisons with model predictions for the launch of a Titan III rocket at the Air Force Eastern Test Range are presented in this report, along with a limited amount of airborne sampling measurements of other cloud species (O_3, NO, and NO_x). The measurement activity was conducted as part of a continuing NASA program with joint participation by the Langley Research Center, Kennedy Space Center, and Marshall Space Flight Center.

Although the sampling instrument array was not ideally located for maximum effluent measurements, values above background levels for exhaust constituents were obtained at surface level for 3 of the 5 primary or manned instrument sites, which were located at sea, and 17 of the 25 secondary or unmanned sites, located on land. No levels exceeded currently accepted public health standards. The exhaust cloud split into more than one component, with the major cloud being optically tracked for 22 min after launch. Comparison of this launch with earlier launches indicates cloud rise rate was the same, cloud stabilization altitude was higher, and cloud volume was nearly twice as large as previously measured.

Postlaunch model prediction of cloud path and effluent dispersions using meteorological data near launch time are presented. Cloud path and rise rate predictions compared well with the measured results. Cloud stabilization altitude differed significantly (attributed to insufficient meteorological data) and effluent concentration predictions were higher than measured values.

The results of this experiment established the need for additional meteorological data for future missions to aid in site selection for sampling instruments, data analyses, and comparing model predictions with measurements.

INTRODUCTION

The National Aeronautics and Space Administration is actively engaged in studies to determine the effects of rocket motor firings on the environment in compliance with the National Environmental Policy Act of 1969. These studies are designed to obtain data for vehicles with solid-fuel rocket motors to be used in the establishment of potential launch constraints using model prediction techniques and to develop expertise in the areas relating to the environmental impact of launch activities. The approach employed to meet these objectives

is to measure the concentration and dosage of exhaust effluents produced by large solid-fuel rocket motors, both at the surface and within the rocket exhaust cloud, and to optically record the physical growth of the cloud. Finally, the surface measurements are compared with diffusion model predictions to assess the effectiveness of the model, and the airborne measurements are used to assess model source-term estimates.

During the launch of solid-fuel rockets, exhaust effluents such as HCl, Al_2O_3, CO, CO_2, and possibly other species are formed in a visible cloud at potentially toxic levels (ref. 1). The buoyant cloud rises and entrains (and reacts with) large quantities of ambient air. The cloud rises to a stabilization altitude, theoretically between 500 to 3000 m, which is basically dependent upon the heat content of the cloud and the height of the local atmospheric mixing layer. When the cloud approaches its maximum altitude, it is termed a "stabilized ground cloud." After stabilization the cloud continues to grow while some exhaust effluents disperse to the ground.

Marshall Space Flight Center has developed a diffusion model (ref. 2) to determine the atmospheric transport and ground-level deposition of the exhaust effluents from the stabilized ground cloud. A joint effluent measurement program conducted by Langley Research Center, Marshall Space Flight Center, and Kennedy Space Center has been established with the goal of assessing the effectiveness of the diffusion model predictions and to provide source-term data for the model.

The purpose of this report is to present the results from the launch of a Titan III (ATS-F) on May 30, 1974. The launch occurred at 1247 UT (0847 EDT) at the Air Force Eastern Test Range. The specific objectives of this measurement operation were to (1) measure the concentration and dosage of HCl, Al_2O_3, CO, and CO_2 deposited at surface level beneath the path of the ground cloud and (2) determine the growth history of the cloud. Measurement results from other Titan III launches are presented in references 3, 4, and 5.

In addition, in-cloud concentrations of NO, NO_x, and O_3 were measured using an in-situ sampling system onboard a general aviation aircraft under the direction of the University of Maryland. The primary purpose of these measurements was to obtain data to aid in the assessment of potential stratospheric catalytic destruction of ozone caused by chemical reactions of exhaust products from solid-fuel rocket motors. However, these airborne measurements may also be used to provide the rationale for determining the distribution of other exhaust constituents (e.g., HCl, Al_2O_3) within the cloud and provide information about the physical characteristics of the cloud, both of which are required as inputs for the diffusion model. A description of the airborne measurement system, a discussion of the chemical processes, and a discussion of the primary measurement results are included in reference 6.

Certain manufacturers are identified in this paper in order to specify adequately the instruments used in the research effort. In no case does such identification imply recommendation or endorsement of the instrument by NASA, nor does it imply that these instruments are necessarily the only ones available for the purpose. In many cases equivalent instruments are available and would probably produce equivalent results.

SYMBOLS AND ABBREVIATIONS

AFETR	Air Force Eastern Test Range
DIF	dual isotope fluorescence
KSC	Kennedy Space Center
LC	launch complex
LCU	landing craft utility, an air sampling instrument platform
MSFC	Marshall Space Flight Center
NAA	neutron activation analysis
P	primary instrument set or site
ppb	parts per billion by volume
ppm	parts per million by volume
Q_I	heat release into exhaust cloud, J/kg
RCC	range control console
S	secondary instrument set or site
s	standard deviation
T	time of launch
UCS	universal camera site
$\bar{x}$	mean

PROGRAM DESCRIPTION

Launch Vehicle

The Titan III launch vehicle was developed by the United States Air Force for space launches at the Air Force Eastern and Western Test Ranges. The launch vehicle consists of a three-stage core using a liquid-propellant propulsion system and two solid-fuel rocket motors (stage 0) attached on opposite sides of the core. Stages I, II, and III are ignited above the troposphere; only stage 0 with the two solid-fuel rocket motors contributes effluent to the ground cloud. Each solid-fuel motor is approximately 3 m in diameter, 26 m tall, and weighs 2.3×10^5 kg. The two solid-fuel rocket motors develop more than 7 MN of thrust at lift-off. The solid propellant consists of an ammonium perchlorate oxidizer, aluminized synthetic-rubber binder fuel, and various other additives to stabilize mass and to control the burning rate.

The potentially toxic exhaust effluents emitted by the stage 0 solid-fuel rocket motors include hydrogen chloride, aluminum oxide, and carbon monoxide and chlorine. The quantity of vehicle exhaust contributing to the formation of the ground cloud is calculated on the basis of the stabilization altitude of the cloud, the trajectory of the vehicle, and the burn rate of the motors. (See refs. 2 and 7.) The approximate weights of the significant exhaust products (from ref. 3) comprising the ground cloud are shown in table I. A detailed discussion of the composition of the exhaust at the rocket motor's exit plane and downstream of the exit, including the effects of afterburning, is presented in reference 8.

Field Operations

For launch vehicle effluent measurement operations, surface-level air sampling instrumentation is deployed using trucks or seacraft which have to be positioned several hours prior to launch. Estimates of cloud path direction must be available in sufficient time (T - 12 hr) to allow for instrument site selection, travel to the site, instrument loading (for sea operations), instrument checkout and calibration, the obtaining of background (ambient air) data, and range safety considerations.

For this measurement operation, all five manned (primary) instrumentation sets were deployed at sea and 25 unmanned (secondary, fallback zone, or tower) instrumentation sets were deployed on land. Primary instrumentation sets were operated by two instrument technicians at each site who were in radio communication with the principal investigators located at the AFETR control center. The unmanned instrumentation sets were activated and deactivated remotely from the RCC.

Cloud path and effluent concentration predictions.- The deployment of all surface-level instrumentation is keyed to the predictions of the direction of cloud travel (cloud path) and effluent concentration, which in turn are dependent upon accurate meteorological profiles for the thermodynamics and kinematics of the atmosphere. Local temperature, pressure, and wind velocity as a function of altitude serve as inputs to the dispersion model (ref. 2), which is used to predict probable cloud path and effluent concentrations. A team from MSFC was responsible for providing meteorological forecasts (from data supplied by the U.S. Air Force Air Weather Service) and effluent predictions. Application of the NASA/MSFC Multilayer Diffusion Model for real-time cloud dispersion predictions is discussed in detail in reference 9. Prelaunch forecasts of cloud path and effluent concentrations are included in table II and are based on the meteorological data included in reference 10.

Instrumentation location.- Initial instrument site selection is nominally made 12 hours prior to scheduled launch and is updated as new meteorological data become available. For this operation, the predicted cloud azimuth at this time was 55.1° with peak effluent concentrations predicted to occur 3.3 km from the launch site. (See table II.) This prediction dictated total sea deployment for all five primary instrumentation sets (designated P-1 to P-5) and the

deployment of all 25 secondary instrumentation sets between the launch site and the ocean. By T - 8 hr all seacraft had been loaded and departed from the docks with instructions to proceed in a direction north of the rocket vehicle azimuth. The T - 8 hr effluent dispersion prediction indicated a cloud azimuth of 55.5° and a peak effluent concentration at 4.4 km from the pad. The boat captains were radioed to proceed to sampling positions, as shown in figure 1, based on these predictions. Seacraft position assignments were based on instrument effluent detection capabilities, seacraft characteristics, and weather stability. The nominal sampling station for P-2 was near the predicted region of peak effluent concentration. Since the desired sampling station for P-2 was within a prelaunch restricted zone, P-2 was positioned at a holding station outside the restricted zone with instructions to proceed to the desired sampling location 90 sec after launch, when all zonal restrictions would be lifted.

A pronounced southerly shift in the winds at altitude between the T - 8 and T - 5 hr soundings caused the counterclockwise shift in cloud path prediction at T - 5 hr from an azimuth of 55.5° to 37.6° (table II). New seacraft locations were calculated based on this information but were not implemented because, by the time these calculations were completed, additional meteorological data indicated the cloud path would shift clockwise (back toward the south). The T - 2 hr meteorological data confirmed this shift and, consequently, new seacraft positions were determined. As shown in figure 1, the seacraft were directed to new holding and/or sampling locations, based on a sampling array centered about an 81° cloud path. The seacraft maintained these positions until launch, after which they were directed to a series of new positions based on real-time observations of the direction of cloud travel. The seacraft positions shown in figure 2 represent the final primary instrumentation locations. Positive launch effluent data were obtained at both locations shown for P-2. Also shown are the unmanned instrument set locations and the paths traveled by the exhaust clouds (to be discussed).

The nominal deployment strategy for the unmanned secondary instrument sets is to create an array which will both extend beyond and fill in the gaps between the primary instrument sets. However, for seaward drifting clouds originating from LC 40, this strategy becomes difficult to implement without a sizable (and costly) increase in the number of seacraft. The alternate scheme employed for this operation was to deploy the secondary sets approximately 150 m apart along the only road between the launch pad and the ocean. Approximately half of the sets were deployed north and the other half south of the predicted cloud path. The secondary instrument sets are battery powered, but other unmanned sets require alternating current and must be located at fixed power sites. These were located at sites AA, DD, EE, and FF, as shown in figure 2, and were positioned based on the T - 8 hr cloud path prediction. Site coordinates for all instrumentation are listed in table III. Instrument site locations are estimated to be accurate within ±100 m. Instruments at site AA were located approximately 7 m above the ground, all other unmanned instruments were near 2 m above the ground, and all manned instrument sets were within 3 to 5 m above sea level.

Measurement Systems

The desire of the modeling community to test diffusion models for various meteorological phenomena dictated the formation of a wide variety of simple and complex instruments overlapped into a network of surface (land and sea) and airborne instrumentation systems. With these requirements and the uncertainty in wind direction and cloud stabilization height, one is soon involved with a rather large and complex measurement system. The two exhaust cloud constituents of most interest to the modelers are HCl gas and Al_2O_3 particles; thus, a simple division of the measurement system follows along these lines. Another division is between those instruments which are normally manually operated, defined as primary instruments, and those operated by remote control, defined as secondary, fallback zone, and tower instruments. Model requirements of cloud rise rate and growth pointed to some type of photographic record and this was fulfilled by using the existing optical tracking and time-sequence camera systems at the AFETR.

Optical system.- Three Askania optical tracking cameras were employed to record the movement of the ground cloud from formation until dissipation. Camera characteristics are discussed in reference 11 and the camera locations are shown in figure 3. The tracking camera data were used to calculate the approximate location of the cloud centroid in three-dimensional space as a function of time. The three cameras were synchronized, giving the cloud location at 10-sec intervals. In addition to the tracking cameras, a Hasselblad time-sequenced camera was placed at each tracking camera site to obtain color photographs of the cloud every 15 sec from launch to T + 5 min and at 1-min intervals thereafter. These photographs were used to document cloud formation and growth.

Manned sampling system.- The primary or manned instrument sets were composed of those instruments listed in table IV. Sites P-1, P-2, and P-3 were arranged along the predicted ground track of the cloud centroid, the region of maximum effluent concentration, and thus were the most heavily instrumented. Instrument capabilities based on laboratory and field experience or from manufacturers' data are listed in table V, and further descriptions of these instruments are given in references 12, 13, and 14. Particle analysis was directed at (1) the identification of chemical elements and their relative abundance using neutron activation analysis, (2) the determination of mass loading in the respirable size range using gravimetric analysis, and (3) the determination of particle size using microscopic counting techniques. Appropriate background samples were taken prior to launch using selected instruments and are discussed in the section entitled "Results and Discussion."

The nominal prelaunch schedule called for checkout of the instruments beginning at T - 4 hr, followed by a functional check, and then on-site calibration of the chemiluminescent detector, microcoulometer, and CO_2 analyzer. CO and CO_2 calibration gases were used in the calibration processes. During the same time period, the particle instrument system operator turned on the mass monitor (but not the associated recorder) for functional tests. At T - 1 hr all systems (except bubblers and filter collectors) were activated for 30 min of background data. At T - 30 min all instruments were placed in a launch readiness mode until launch. For launch operation where launch delays

occur after instrument set deployment, the instruments are recalibrated and additional background data acquired on a selective basis. After launch, the instruments were activated and later deactivated on a schedule depending on predictions of cloud stabilization altitude and velocity to allow for minimum contamination from other sources. Potential inaccuracies in calculating cloud arrival and departure times were considered in determining instrument activation and deactivation times to insure that no data were missed. Typically all instruments are visually monitored from 15 to 60 min after launch. Outside of this time period, the operators were instructed to immediately activate all instruments at the first sign of launch effluent (e.g., visual observation, odor, pH paper discoloration). Additionally, all instruments were left in the operational mode until the readings returned to either background or prelaunch levels. After receiving approval from the cognizant principal investigator located at the RCC, the operators postcalibrated the gas detection instruments and ran another background sample on the particle mass monitor. The particle instrument operators at P-1, P-2, and P-3 had a light-scattering photometer to measure particle size distribution. Measurements were obtained at 1-min intervals after launch until the site was deactivated.

Unmanned sampling system.- There were 25 remotely operated instrument sets deployed. The instrument complement for each set is listed in table IV. Each site designated by the prefix S (for secondary) included a bubbler with pump and pH paper for the detection of HCl and a Nuclepore filter (47 mm diameter) with pump for the detection of particles. Figure 4 is a photograph of a typical secondary site. Sites S-100 and S-101 were equipped with two bubblers and two filter systems. In general, however, one HCl bubbler system and one filter system were combined with a radio-controlled instrument activation system (ref. 15) to comprise a complete secondary site. All instruments at a site were activated and deactivated simultaneously on radio command from the AFETR control center. Activation and deactivation times were determined from diffusion model predictions of exhaust cloud arrival and departure times over a site with some margin allowed for prediction errors. These times were modified for some instrument sites based on real-time data from the manned sites.

The HCl detection bubblers draw ambient air through the system at a nominal rate of 3 liters/min. Each bubbler was filled with 20 cm^3 of distilled water. The resultant sample was removed and analyzed, using a coulometric technique for chloride analysis, within 24 hr after the mission sampling period was completed. The particle detection system consisted of a filter supported by a plastic holder and oriented so that the ambient air entered the system horizontally. The filters were weighed at Langley before and after the mission in a class 100 clean room after allowing the samples to equilibrate to clean-room conditions. The filters were preset for a flow-through rate near 28 liters/min and checked after launch.

RESULTS AND DISCUSSION

Optical Measurements

Tracking cameras.- The centroid of the ground cloud was tracked by three tracking cameras for 22 min after launch. After this time the exhaust cloud

could not be distinguished from the natural cloud background and tracking inconsistencies began to increase. Ground track of the cloud is shown in figure 5. Cloud position was determined to be the center of the triangle formed by the intersection of each pair of camera azimuth angles (for ground track) and elevation angles (for altitude). The error bars represent the distance from the determined cloud position to the furthest of the three intersection points. Part of this error is attributed to the selection of the different cloud centers by the various camera operators. The camera sites are widely separated, each operator sees a different view of the cloud, and vision may be hindered to different degrees by haze and natural cloud background. Position of the cloud as a function of time from launch is also indicated in figure 5. Near T + 3 min it became apparent to the ground observers that the cloud was splitting into two major components, one moving in an easterly direction and the other in a southeasterly direction. The cameras tracked the southeasterly moving cloud, which was the larger and more dense of the two clouds.

Between T + 3 min and T + 6 min, this entire cloud had crossed the land/ocean interface and a southerly shift in cloud direction occurred. This phenomenon has since been observed for other launch clouds and has prompted the inclusion of constant-altitude balloon (tetroon) releases prior to subsequent launch vehicle effluent measurement activities. The tetroons were released at times and launch points and inflated to attain altitudes best simulating predicted cloud behavior to aid in the positioning of effluent measurement instrumentation. The shift in cloud path direction may be attributed to local atmospheric turbulence caused by thermal differences between land and sea which results in atmospheric eddies. The measured track of the southeast cloud and the path of the east cloud, estimated from seacraft personnel observations, are shown in figure 2 along with final instrument locations.

Cloud rise as a function of time from launch is shown in figure 6. The error bars are about the same magnitude as determined for other measurement operations. (For example, see ref. 3.) Also shown is the ambient temperature variation as a function of altitude. Cloud rise is compared with measurements from two previous Titan III launches in figure 7. Although rising to different stabilization altitudes, which is a function of the atmospheric thermodynamic structure, all clouds exhibited rise rates to stabilization altitude near 4.8 m/sec.

Time-sequenced cameras.- Photographs of the southeasterly drifting cloud taken from the three camera sites were used to determine cloud volume history according to the techniques described in reference 4. As shown in figure 8, cloud volumes were determined from launch to T + 6 min. The upper curve is a fairing of the data obtained using approximately 30 photographs from each of two camera sites (UCS-9, UCS-2), while the lower curve is from another pair of sites (UCS-9, UCS-26). Data from the remaining pair of camera sites if plotted (UCS-2, UCS-26) would be encompassed by the envelope formed by the two curves shown in the figure. Cloud volumes obtained from any pair of cameras are estimated to be accurate within 20 percent. The inflection points in the curves occur near T + 3 min, which is about the time of the cloud split into two pieces near the land/ocean interface. In figure 9, the average of the cloud volume data from figure 8 is compared with similar data from an earlier Titan III launch (Feb. 11, 1974) which is discussed in reference 4. The

February 1974 cloud data also exhibit an inflection near the land/ocean interface. The average volume growth rate for the two clouds differ by nearly a factor of two during the first 3 min after launch but are similar after 6 min. These data, along with similar data from other launches, will serve as inputs to diffusion models requiring assumptions of cloud volume at stabilization and volume expansion rate after stabilization.

By knowing the volume history of the cloud, the relationship between the mass of rocket exhaust products and ambient air (mass dilution ratio) can be determined. The mass and composition of the exhaust products may be calculated at the exit plane with high confidence and may be estimated at later times provided such parameters as cloud temperature, constituent chemical reaction rates, and the quantities and composition of nonexhaust constituents entrained within the cloud can be determined. The mass dilution ratio for the May 1974 exhaust cloud has been determined and is shown in figure 10. Also shown is relative humidity obtained during sampling aircraft penetrations of the cloud.

Surface Effluent Measurements

Background sampling for HCl, CO, and CO_2 was conducted from T - 1 hr to launch. Ambient HCl and CO concentrations were below 0.05 ppm and 0.5 ppm, respectively (these being the lower detection limits of the instrumentation as determined for this operation), and agree with previous measurements (refs. 3 and 4). No background particle loading was obtained but has been typically 20 to 30 $\mu g/m^3$ for earlier operations. CO_2 concentrations were near normal background values (320-340 ppm). All data presented in this report, with the exception of particulate data, have been adjusted for background measurements. The concentration of ambient sodium chloride was determined to be below the average chloride concentration of the bubbler water and, consequently, was disregarded as an interferent with HCl measurements from the bubbler. No particulate data definitely attributed to launch were recorded at any primary site except for the Nuclepore filter measurements at site P-4 (to be discussed). Final instrument site locations are shown in figure 2 and site coordinates are listed in table III.

Manned sites.- As seen in figure 2 only the P-1 seacraft was able to achieve a position near the southeasterly drifting (major) cloud. Therefore, all measurement data from the remaining seacraft are attributed to fallout from the easterly drifting cloud. The P-2 seacraft is shown at two locations because launch effluents were measured at both positions. No bubbler (HCl detector) dosage at any primary site was above the 80 ppm-sec detection limit of the sampling system although bubbler data above this value were obtained at some of the unmanned sites (to be discussed).

The primary site P-1 was located approximately 9.5 km and on an azimuth of 108° from the launch pad and an estimated 0.5 km north of the center of the southeast cloud at the time of cloud passage. All instruments functioned normally, although radio transmissions from the seacraft affected instrument readings. The highest HCl measurement recorded on the chemiluminescent instrument was 0.05 ppm, the lower detection limit of instrument. Also, no pH paper color changes occurred. In addition, no CO measurements were recorded above the

minimum detection limit of the instrument (0.5 ppm). No particulate measurements attributed to the ground cloud were recorded by the instruments at this station.

Significant positive data were recorded aboard the P-2 seacraft at and between the two measurement sites shown in figure 2. Estimates of HCl concentrations above background were determined from the microcoulometer operated by Brooks Air Force Base personnel. The microcoulometer output is a direct measure of the total chloride sampled. To obtain HCl concentrations some assumption as to the distribution (with respect to time) of the incoming sample (in this case HCl) must be made. Using the techniques of reference 13, Brooks AFB personnel estimates of HCl concentrations above background from about T + 19 min to T + 45 min are presented in figure 11. A peak value near 1.3 ppm was determined to occur near T + 23 min. The microcoulometer measurement times compare favorably with the increase in voltage output from the chemiluminescent detector aboard the seacraft. However, the pulse type response obtained by the chemiluminescent detector for this operation precludes accurate quantification, so no data are included in this report. The spiked pulses are attributed either to (1) unstable instrument response, which is an instrument malfunction induced either by the automatic mode under which the instrument was operated or HCl/particulate interference (or both), (2) operator error, or (3) radio interference. Instrument operators aboard the seacraft reported the edge of the (easterly) exhaust cloud to be nearly overheard from T + 19 min to T + 23 min during which time a mist was observed around the seacraft. The mist was apparently not highly acidic since no color changes occurred on the pH paper onboard the seacraft and no physical effects were reported by personnel onboard the boat. Due to operator error, the bubbler (HCl detector) was not operating during the periods when the microcoulometer measured HCl. The measurements from the particle mass monitor during this time period were characterized by spikes that only intermittently went above the normal background level and therefore are considered insignificant.

After cloud passage, the P-2 seacraft was directed to a more easterly location (see fig. 2) in an attempt to reintercept the cloud. No instruments were turned off during the repositioning operation. One operator reported that his particle instrument (mass monitor) was measuring seacraft exhaust fumes near T + 27 min. HCl measurements above ambient were once again recorded by the microcoulometer after arrival at the second measurement site (approximately T + 32 min) and are shown in figure 11. However, the measurements are less than 1 ppm, which is near the detection limit of the instrument and may not indicate the presence of launch effluents. No mist or color changes in the pH paper were observed at the second measurement location.

CO measurements were also made aboard the P-2 seacraft and are shown in figure 12 as a function of time from launch. CO increased above ambient (0.5 ppm) near T + 19.5 min, reached a maximum of about 5.5 ppm near T + 23 min, and returned to prelaunch background levels around T + 44 min. The high amplitude oscillations in the data may reflect CO diffusion from the cloud but also may be caused by intermittent sampling of the ship's exhaust, since the engines were not shut down during this time period. A comparison of the CO and HCl data traces (figs. 11 and 12) shows that measurements above ambient for the two species began (T + 19.5 min), peaked (T + 23 min), and ended (T + 44 min)

near the same time, indicating that at least part of the CO measured originated in the ground cloud. However, the HCl values returned to ambient approximately 3 min after observed cloud passage over the first measurement site (T + 23 min) and increased only slightly (still below the normally accepted detection limit) after the second measurement site was reached, whereas the CO values returned to ambient only after the cloud had passed over the second measurement site. Sampling of the ship's exhaust probably accounts for these differences. The particle sampling mass monitor recorded spikes reaching about 140 $\mu g/m^3$ at T + 30 min. It is not known if these spikes were from the cloud or were fumes from the ship's engine. In addition, the Nuclepore filter from this station shows no increased mass loading above background.

No positive data were recorded on the instruments at P-3. The P-3 seacraft, an LCU, is a slow moving ship which attempted to reach the southeast cloud and did not arrive at the position shown in figure 2 until after passage of both clouds. In addition, the P-3 seacraft served as a communication ship between the personnel directing the mission on shore and the instrument operators at sea. Significant sampling instrument interference was noted during the frequent radio transmissions which may have precluded any sampling of the easterly drifting cloud.

No chemiluminescent HCl detector was located aboard the P-4 seacraft; however, a visible mist was observed around the seacraft for 4 to 5 min (beginning near T + 42 min), corresponding to the period when the cloud was overhead. The instrument operators reported a stinging sensation in their eyes during the same time period, indicating that the mist was probably acidic. Further evidence of this is indicated by the spotted discoloration of the pH paper onboard the P-4 seacraft as shown in figure 13. The mass monitor at P-4 measured no significant increase during the time period when the mist was reported. However, analysis of the Nuclepore filter showed heavy mass loading (288 $\mu g/m^3$) of which 30.7 µg were determined to be aluminum. These data, along with the Nuclepore filter data from the other primary sites, are shown in table VI. Included are (1) total mass, obtained from weighing of the filters, (2) total mass loading, which accounts for sample flow rate, (3) the masses of Al and Cl, determined from neutron activation analysis (ref. 16), and (4) Al mass loading. Applying the results of the statistical analysis (see appendix) of the particulate data obtained at the unmanned sites (to be discussed) only the measurements at site P-4 are attributed to launch effluents. No CO measurements above background were recorded at P-4.

The results from P-5 were similar to those of P-4 in that a mist was sensed during a 4- to 5-min period (beginning at T + 28 min) when the cloud was overhead, and the pH paper developed spotting (see fig. 13). (As was the case with seacraft P-4, there was no chemiluminescent HCl detector onboard P-5.) In addition, positive CO data traces were obtained, as shown in figure 14, indicating increases above ambient (0.5 ppm) starting near T + 22 min and continuing through T + 31 min, after which an instrument malfunction occurred. As shown in the figure, maximum values of CO near 2 ppm above ambient were measured from 26 to 30 min after launch.

The particle sampling mass monitor results from P-5 are shown in figure 15. The average background particle loading prior to cloud arrival over

the site was 10 $\mu g/m^3$, and values started to increase above ambient near T + 23 min. The rapid increase and decrease between T + 30 min to T + 31 min is believed to be caused by a significantly large liquid mass hitting the sensing crystal which subsequently evaporated, resulting in a mass loss. The reading at T + 36 min is interpreted as being caused by primarily a solid rather than liquid mass, since it is not characterized by a sharp drop below ambient levels. These high particle loading spikes, although above the normal background, do not exceed currently accepted health standards since they occur for relatively short time intervals.

In summary, positive launch effluent measurements were obtained at three of the five primary instrument sites; however, these measurements were not beneath the major exhaust cloud. HCl, CO, and particulate values were measured above background levels but not at levels exceeding currently accepted public health standards.

Unmanned sites.- The 25 unmanned remotely operated sets of air sampling instrumentation were placed between the launch pad and point of cloud stabilization and thus were not in regions of expected high effluent dosages. The instruments at site AA failed to function due to a loss of power, and the particle instruments at sites S-102 and S-106 malfunctioned. HCl measurement results, corrected for background, for the remaining instrument sets are shown in table VII. The minimum detection limit of the HCl instruments is 80 ppm-sec. Particle measurement results are shown in table VIII. Concentrations of Al and Cl shown in the table were obtained from neutron activation analysis. All sites providing loadings above 50 $\mu g/m^3$, the usual background value for the KSC area, could have recorded launch effluents. However, since most of the sites were adjacent to roads and subject to vehicular traffic contamination, the results of neutron activation analysis (ref. 17) of the particle filters were used to determine if any launch effluents were present. Only those six sites having Al mass loadings beyond two standard deviations from the mean of the Al mass loading measurements as obtained by neutron activation analysis are believed to have recorded launch effluents. The rationale of this approach is discussed in the appendix.

The relative location of the unmanned instrument sets and the random pattern of the positive effluent measurements (HCl and Al) are shown in figure 16. Also shown in the figure are the initial cloud path and surface wind direction. Four out of five sites in a group north of the pad (sites S-106 to S-110 and DD) measured HCl dosages above the 80 ppm-sec minimum detection limit (see table VIII). Dosages decreased as site distance from the pad increased. However, one site (S-107) in the group recorded no data which can be attributed to launch and only one site (S-110) provided both HCl and particulate measurements above background. Sites S-102 and FF were close together and provided HCl measurements above background, although neither site measured particulates. The highest HCl measurement (358 ppm-sec) was made at site EE. This value is unusually high considering that no hydrogen chloride above background was recorded at nearby sites S-100, S-101 (each equipped with two bubblers), and S-202. Significant particle data were measured at only one of the two sets located at site S-101 and no particle data from the two sets at site S-100. In addition, one bubbler at nearby site S-201 measured a dosage of only 135 ppm-sec, while the second bubbler at the site recorded no values above the

minimum detection limit. Particulate measurements were recorded at sites S-203 and S-204, the two sites closest to the measured cloud track. Neutron analysis indicated the highest Al mass loadings were obtained at those two sites. The only evidence of HCl was an acidic spot on the pH paper at site S-204 (fig. 13). Neutron activation analysis indicated extremely high amounts of chlorine at site S-205 but only a less than average amount of aluminum. Three of the four most southern measurement sites (S-207, S-208, and S-210) recorded HCl while the fourth (S-209) measured nothing above background. Particulates were measured at site S-206 and an acidic spot appeared on the pH paper at site AA (fig. 13), the closest site to the launch pad.

From the measurements at the unmanned sites, there is little doubt that launch effluents are diffusing to the ground in the vicinity of the launch pad. However, for this particular launch, the HCl dosages measured were below minimum acceptable public and occupational standards (ref. 1) although higher dosages may have reached the ground at uninstrumented areas. In addition, other meteorological conditions could have caused higher HCl dosages to be measured at ground level. No definite relationships can be identified coupling combinations of cloud path, surface wind direction, or measurement site distance with quantities of effluents measured. Most HCl measurements were recorded at sites furthest from the cloud path and surface wind vector. Conversely, most particle measurements were at a group of sites near the pad in the direction of the surface wind vector and in a downstream direction from the pad flame trench (Azimuth = 101°). Some sites recorded HCl above background measurements but no corresponding particulate measurements, while others recorded particulates but no HCl. No single site recorded positive signs of launch effluents on all instruments at the site.

Another consideration is that the wind direction data (fig. 17) indicate that little, if any, exhaust effluents could have been transported very far north of the pad. Of course whether or not the wind data are applicable for the region surrounding the launch pad and during the entire measuring period is also open to question. In addition, some of these northern effluent measurements and the randomness of all the unmanned site results may be attributed to local air turbulence possibly enhanced by the hot rocket exhaust cloud. Such a phenomenon could cause significantly different effluent measurements at adjoining sites, particularly for those sites near the launch pad. Also, the particle measurements may be influenced by launch pad debris and the location of the site relative to the pad flame trench. In addition, data from the nonselective, dosage type instruments comprising the unmanned sites are difficult to interpret in the absence of any real-time instruments. For these reasons, the authors require that dosage of HCl and particulates be measured at a given site before those data are conclusively considered as launch effluent measurements. Only sites S-110 and S-210, at the extreme ends of the measurement array, meet this criterion.

Airborne Measurements

In-cloud concentrations of NO, NO_x, and O_3 were measured using an instrumented Cessna 205 aircraft under the direction of the University of Maryland. Determination of surface level toxicity was not the objective of the airborne

measurements, but rather investigation of the potential stratospheric catalytic destruction of ozone caused by chemical reactions initiated by exhaust products of solid-fuel rocket motors. Some pertinent results of these measurements are given in reference 6 along with a discussion of the chemical processes involved. However, in addition to the primary objective of the airborne measurements, the results are also useful in that they provide a rationale for heuristically determining the distribution of other exhaust constituents (e.g., HCl, Al_2O_3) within the cloud and provide information about the physical characteristics of the cloud, both of which are required as diffusion model inputs.

Typical profiles for NO, NO_x, and O_3 (from pass 6) are shown in figure 18. The O_3 profile is a mirror image of NO, and the O_3 depletion results from a very rapid reaction between NO and O_3. Typical background O_3 levels were measured to be 50 ppb in the AFETR area which correspond to the natural levels in the troposphere. The aircraft made eight penetrations of the cloud during the time period from 5 to 34 min after launch at airspeeds from 38 to 43 m/sec. One pass was made outside of the visible cloud. Passes were made in both the downwind and crosswind directions at altitudes from 900 to 1740 m. Measurements of NO_x, NO, NO_2, and cloud width are listed in table IX for each pass. Three distinct clouds were observed to form by the end of pass 2 at altitudes near 1700 m (passes 3, 4, and 5), 1200 m (passes 6 and 7), and 1000 m (pass 9). As previously discussed, surface-level observers were able to distinguish only two distinct clouds. The metric tracking cameras measured the center of the southeasterly drifting cloud to be at altitudes higher than the aircraft was flying between 14 and 22 min after launch (passes 3, 4, and 5). However, considering the metric camera tracking accuracy (see fig. 6), the size of the cloud, the differences in visual perspective, and the aircraft measurement strategy, the difference is not unreasonable.

Beginning with pass 6, aircraft measurements were made through the second cloud at 1200 m altitude. Near this time the P-5 seacraft reported the aircraft passing through a cloud directly overhead (the easterly drifting cloud). Pass 8 was intentionally made at the same altitude but downwind of the visible easterly drifting cloud and above the lowest cloud (penetrated during pass 9). No NO_x was recorded indicating that the gaseous NO_x did not extend beyond the visible cloud by a significant distance. Airborne missions in conjunction with later Titan III launches, in which other cloud constituents were measured, confirm that the gaseous exhaust constituents (and their chemically produced by-products) did not extend significantly beyond the visible cloud.

Model Comparisons

Calculations of cloud path and effluent dispersions were made after the launch using data from meteorological soundings taken near launch time, so that model predictions could be compared with the observed cloud behavior. These calculations were performed by MSFC personnel using the NASA/MSFC Multilayer Diffusion Model (ref. 2). Details concerning general applications of the model and assumptions employed are presented in reference 9. Atmospheric thermodynamic and kinematic conditions used for the analysis are shown in figure 17 and are from the T + 4 min rawinsonde sounding and the launch-time meteorological tower data (ref. 10).

Postlaunch model predictions of cloud path and HCl isopleths at surface level are shown in figure 19 along with the actual cloud path (southeasterly drifting cloud) obtained from the optical tracking cameras. (See fig. 2.) The model-predicted cloud path compares very favorably with the measured data. The prelaunch predictions of more northerly cloud paths are attributed to a lack of sufficient meteorological data to permit accurate cloud path forecasting and, to a lesser extent, to an incorrect assumption concerning Q_I, the heat produced during ground cloud formation, which is a diffusion model input. Initially Q_I was determined to be 2.89 MJ/kg (assuming single-phase flow), a value which was calculated neglecting CO afterburning, and it is this value that was used for the prelaunch predictions shown in table II. The postlaunch model predictions in figure 19 were calculated assuming Q_I = 10.46 MJ/kg, a value supported by empirical results showing cloud stabilization heights usually being higher than predicted, and are derived assuming almost total CO afterburning and some energy losses. Calculations assuming total CO afterburning and no energy losses would require Q_I = 12.13 MJ/kg, a value which would result in higher cloud stabilization altitudes. A detailed discussion concerning the effects of Q_I on cloud path and effluent dispersion predictions is included in reference 17.

The region of peak HCl concentrations, 3.21 ppm, was predicted by the model to occur at 4.54 km from the launch pad at an azimuth of 115° from the pad. This value, along with several isopleths showing predicted HCl concentrations at surface level, is shown in figure 19. Predictions of HCl concentration and dosage at the surface along the ground track of the cloud centroid as a function of distance from the launch pad are shown in figure 20. No measurements were obtained to either confirm or refute these values with the possible exception of the HCl detector at site P-1 which recorded HCl of 0.05 ppm, a value which is at the normally accepted lower detection limit of the instrument. In addition, the P-1 seacraft was in a better position to measure launch effluents from the cloud drifting toward the east rather than for the cloud drifting toward the southeast. It should be pointed out, however, that the measurements made beneath the easterly drifting cloud were lower than the model predictions for the southeasterly drifting cloud.

Cloud centroid altitude as a function of time, obtained from postlaunch model predictions and using launch-time meteorological data, is shown along with optical tracking and aircraft data in figure 21. The tracking cameras followed the southeasterly drifting cloud, which was the largest of the clouds, while the aircraft initially flew through the cloud moving southeast and then through the two easterly moving clouds. From launch to near stabilization altitude model predictions of cloud rise rate compare reasonably well with the optical data. However, a large discrepancy occurs when comparing model predictions of cloud altitude with the optical data for the southeasterly drifting cloud. The data from the aircraft measurements are, on the average, lower than, but within 15 percent of, the optical data, which can be partially accounted for by a difference in visual perspective and measurement strategy, whereas the model predictions differ by nearly a factor of two. The exact reason for this discrepancy is not known at this time, However, the differences may lie in inadequate meteorological data which prevented the model from predicting cloud breakup and subsequent separate cloud paths and stabilization altitudes. Based on the meteorological data available (fig. 18), the cloud

followed by the tracking cameras stabilized above the surface mixing layer as determined by the model. This phenomenon could not have been forecasted by the NASA/MSFC Multilayer Diffusion Model. From these results it was decided that more extensive meteorological balloon releases would be required for future measurement operations.

As shown in figure 21, a better comparison exists between the model predictions and aircraft measurements of altitude for the easterly drifting clouds. In addition, good agreement exists between model predictions and the aircraft measurements prior to T + 8 min. However, these measurements are from the first two aircraft passes when measurement strategy was to penetrate the cloud as soon as possible with less regard to sampling at the cloud centroid.

CONCLUDING REMARKS

All available instrument sets were successfully deployed and, with a few exceptions, successfully operated during the mission. The manned instrumentation sets were deployed at sea. The prelaunch prediction of seaward cloud travel required land deployment of all unmanned instrument sets in a linear array near the launch pad rather than in the desired array filling in the gaps between the manned instrumentation sites located at sea. This did not allow any unmanned instruments to be located in regions of predicted high effluent dosages. Changes in wind direction just prior to launch and range safety restrictions prevented locating the manned instrument sets in the desired positions directly beneath the southeastern exhaust cloud.

However, because the cloud split into more than one piece, effluent measurements were made at the three launch sites located beneath the path of the easterly traveling exhaust cloud. HCl, CO, and particulate values above background were measured during the time of cloud passage but not at levels exceeding currently accepted public health standards. Part of the CO measurements may be attributed to the boat exhaust. A visible mist was observed around two of the seacraft and instrument operators did report a stinging sensation in their eyes, probably indicating the presence of some acidic constituent.

Although effluent measurements above background levels were made at 17 of the 25 unmanned sites, at no site did all instruments at the site record positive launch effluent data. This may be attributed to local air turbulence and the lack of uniform mixing during the early time when the cloud passed over the unmanned sites. In addition, at only two unmanned sites (located at the extreme opposite ends of the measurement array) were both HCl and particulate measurements recorded and one of these sites was located almost 2 km upwind of the launch pad. This apparent inconsistency (although the wind data may not be applicable), coupled with the difficulty of interpreting data from nonselective dosage-type instruments in the absence of data from real-time instruments, precluded any qualitative analysis of the unmanned site data.

The southeasterly drifting exhaust cloud was optically tracked from launch to about 22 min after launch. This cloud appeared to be larger and more dense than the easterly drifting cloud. Cloud rise rate to stabilization altitude was near the 4.8 m/sec value measured for prior launches, although the

stabilization altitude was higher. A shift in direction in cloud travel occurred when the cloud passed over the land/ocean interface, a phenomenon observed during other launches, and is attributed to local atmospheric turbulence. Optical data were used to determine cloud volume for 6 min after launch. The cloud was approximately twice the size of the cloud produced during an earlier launch but nearly the same rate of growth after stabilization.

Airborne measurements were made within the cloud from about 5 to 35 min after launch showing the O_3 profile to be a mirror image of the NO profile as expected because the O_3 depletion results from a very rapid reaction between NO and O_3. Airborne observers reported three distinct clouds rather than the two observed from the ground, and the aircraft results show the cloud centroid to be lower than that measured by the optical tracking cameras. A pass made above one cloud and downwind of another recorded no values above ambient, indicating launch effluents do not extend beyond the visible cloud by any significant distance.

Postlaunch model predictions of cloud path and effluent dispersions were made using meteorological data from near launch time. The predicted cloud ground track and rise rate compares very favorably with the optical data for the southeasterly drifting cloud. However, a large discrepancy occurs between model predictions and measurements of cloud stabilization altitude for the same cloud. Exact reasons for this discrepancy are not known but may possibly be attributed to insufficient meteorological data which prevented the model from predicting cloud breakup and subsequent stabilization of the southeastern cloud above the surface mixing layer. Better agreement exists between model predictions and aircraft measurements of altitude for the easterly drifting cloud.

Effluent measurements were made beneath the easterly drifting cloud, whereas the model calculations of cloud agree with measured data for the southeasterly drifting cloud. For this reason, exact comparisons between model predictions and field measurements of effluent levels cannot be made. However, the measurements made beneath the easterly drifting cloud were lower than values predicted for the southeasterly drifting cloud.

The overall results of this mission indicated the need for additional meteorological balloon releases, which were subsequently included for later launch vehicle effluent measurement operations to aid in the instrument site selection process, data analyses, and model/measurement comparisons.

Langley Research Center
National Aeronautics and Space Administration
Hampton, VA 23665
June 28, 1977

APPENDIX

PARTICULATE FILTER STATISTICAL TREATMENT

When an analysis is conducted on particle data in an experiment such as this one, it may be difficult to decide what is filter loading due to the event (i.e., rocket launch) and what is natural background. During other launch vehicle effluent experiments, sufficient background samples were taken before launch to aid in the postlaunch data analysis. Unfortunately, no background samples were taken with the Nuclepore filter system and, consequently, the elemental composition of the background particulates is not known. A comparison of the aluminum loadings of the particulate measurement filters with background (KSC) aluminum loadings of references 3 and 4 indicates that all the filters deployed at the unmanned sites during this mission could have sampled rocket effluents because of the relatively high levels of aluminum present. However, the lack of any measurements of other launch effluents at these sites and the direction of cloud travel suggest that this conclusion is in error and that, instead, the aluminum background existing during the time of mission is probably higher than that reported in references 3 and 4. Therefore, the following statistical approach was employed to determine which of the filters had high probabilities of containing (aluminum) launch effluents.

The mean $\bar{x}$ and standard deviation s of aluminum mass loading for all 21 filters was calculated. Then the sample size N was decreased by 1 by omitting the heaviest sample, and $\bar{x}$ and s of the remaining 20 measurements were determined. This procedure was repeated until the sample size was reduced to 3. Next, a ratio of the standard deviation to the mean for each sample size was calculated and plotted as a function of sample size, as shown in figure 22. If it is assumed that the entire group of 21 samples were only background (no aluminum from the launch), then a normal distribution would be expected and the successive elimination of a single sample (the heaviest) would have minimal effect on $s/\bar{x}$. However, if among these 21 samples there are a few samples having both background and launch aluminum, then a skewed distribution (towards heavier loadings since launch samples should have more aluminum) would be expected and successive elimination of the heaviest sample would show a significant change in $s/\bar{x}$. In addition, after having eliminated all the samples containing launch effluents, the additional successive elimination of the heaviest sample would have a minimal effect on $s/\bar{x}$. As shown in figure 22, this successive elimination process does show a significant change in $s/\bar{x}$ for the first 5 or 6 samples, suggesting that these 5 or 6 samples (heaviest) have some aluminum from the launch. To determine the exact point at which the launch samples have been eliminated, the change in the ratio of the standard deviation to the mean ($\Delta s/\bar{x}$) is also shown in figure 22. For sample sizes less than 15, the successive elimination processes have little effect on $s/\bar{x}$. Thus, it is concluded that the 6 heaviest filters sampled some aluminum from the launch, while the remaining 15 samples are background samplings only.

To add additional credence to this technique, a histogram of aluminum mass loading, constructed by plotting the numbers of measurements in successive 2 $\mu g/m^3$ increments, is shown in figure 23. Presented in this manner, the lower range data appear to be normally distributed while the three heaviest measure-

ments belong to a different data set (assumed launch samples). The problem remaining is to determine the number of samples included within the lower range data that also contain launch samples. Using the value of $\bar{x}$ and s for $N = 15$ (the value previously assumed to contain only background samples), the three heaviest samples in the lower range data fall beyond two standard deviations, which suggests that they also contain launch effluents.

Based on this statistical treatment of the data, the six heaviest loaded filters are considered to contain aluminum from the launch cloud and are treated as such in the body of this report.

REFERENCES

1. Environmental Statement for the Space Shuttle Program - Final Statement. NASA TM X-68541, 1972.

2. Dumbauld, R. K.; and Bjorklund, J. R.: NASA/MSFC Multilayer Diffusion Models and Computer Programs - Version 5. NASA CR-2631, 1975.

3. Gregory, Gerald L.; and Storey, Richard W., Jr.: Effluent Sampling of Titan III C Vehicle Exhaust. NASA TM X-3228, 1975.

4. Stewart, Roger B.; Sentell, Ronald J.; and Gregory, Gerald L.: Experimental Measurements of the Ground Cloud Effluents and Cloud Growth During the February 11, 1974, Titan-Centaur Launch at Kennedy Space Center. NASA TM X-72820, 1976.

5. Gregory, Gerald L.; Wornom, Dewey E.; Bendura, Richard J.; and Wagner, H. Scott: Hydrogen Chloride Measurements From Titan III Launches at the Air Force Eastern Test Range, FL 1973 Through 1975. NASA TM X-72832, 1976.

6. Pellett, G. L.: Washout of HCl and Application to Solid Rocket Exhaust Clouds. Precipitation Scavenging (1974), ERDA Symposium Series, No. 41 (CONF 741003), June 1977, pp. 437-465.

7. Hart, Williams S.: Predictions of the Terminal Altitude and Size of Large Buoyant Clouds Generated by Rocket Launches. SAMSO-TR-70-207, U.S. Air Force, May 1970. (Available from DDC as AD 707 110.)

8. Gomberg, Richard I.; and Stewart, Roger B.: A Computer Simulation of the Afterburning Processes Occurring Within Solid Rocket Motor Plumes in the Troposphere. NASA TN D-8303, 1976.

9. Stephens, J. Briscoe; and Hamilton, P. A.: Diffusion Algorithms and Data Reduction Routine for Onsite Launch Predictions for the Transport of Titan III C Exhaust Effluents. NASA TN D-7862, 1974.

10. Stephens, J. Briscoe; Adelfang, S. I.; and Goldford, A. I.: Compendium of Meteorological Data for the ATS-F Launch in May 1974. NASA TM X-73336, 1976.

11. Ehling, Ernest H., ed.: Range Instrumentation. Prentice-Hall, Inc., c.1967.

12. Gregory, Gerald L.; Hudgins, Charles H.; and Emerson, Burt R., Jr.: Evaluation of a Chemiluminescent Hydrogen Chloride and a NDIR Carbon Monoxide Detector for Environmental Monitoring. 1974 JANNAF Propulsion Meeting, Volume I, Part II, CPIA Publ. 260 (Contract N00017-72-C-4401), Appl. Phys. Lab., Johns Hopkins Univ., Dec. 1974, pp. 681-704.

13. Reyes, Robert J.; Miller, Richard L.; and Beatty, David C.: Monitoring of HCl From Solid Propellant Launch Vehicles. 1974 JANNAF Propulsion Meeting, Volume I, Part II, CPIA Publ. 260 (Contract N00017-72-C-4401), Appl. Phys. Lab., Johns Hopkins Univ., Dec. 1974, pp. 705-722.

14. Hulten, William C.; Storey, Richard W.; Gregory, Gerald L.; Woods, David C.; and Harris, Franklin S., Jr.: Effluent Sampling of a Scout "D" and Delta Launch Vehicle Exhausts. NASA TM X-2987, 1974.

15. Radio-Controlled, Sound-Operated Switch. NASA Tech Brief B74-10143, Sept. 1974.

16. Kruger, Paul: Principles of Activation Analysis. John Wiley & Sons, Inc., c.1971.

17. Stewart, Roger B.; and Grose, William L.: Parametric Studies With an Atmospheric Diffusion Model That Assesses Toxic Fuel Hazards Due to the Ground Clouds Generated by Rocket Launches. NASA TN D-7852, 1975.

TABLE I.- TOTAL WEIGHT[a] OF EXHAUST PRODUCTS FROM ZERO STAGE OF THE TITAN III

Effluent	Weight for cloud stabilization altitude near 300 m, kg (b)	Weight for cloud stabilization altitude near 1400 m, kg (c)
HCl	9 500	19 900
H_2O	3 300	7 500
CO	12 900	25 900
CO_2	1 200	2 900
Al_2O_3	15 400	29 300

[a]No plume afterburning is assumed.

[b]Only the exhaust constituents produced during the first 10 sec of zero-stage burn contribute to the exhaust cloud.

[c]Only the exhaust constituents produced during the first 21 sec of zero-stage burn contribute to the exhaust cloud.

TABLE II.- EFFLUENT DISPERSION PREDICTIONS

Time before launch, hr	Cloud stabilization altitude, m	Cloud path from LC 40, deg	Peak HCl concentration, ppm	Location of peak from LC 40, km
24	774	74.7	2.1	3.3
12	764	55.1	2.2	3.3
8	784	55.5	2.2	4.4
5	764	37.6	3.5	4.4
2	764	80.9	3.5	4.4

TABLE III.- SURFACE EFFLUENT SAMPLING STATION COORDINATES

Site designation	Azimuth from LC 40, deg	Distance from LC 40, km
P-1	108.0	9.90
[a]P-2	81.0	5.20
[a]P-2	92.5	10.40
P-3	97.5	10.30
P-4	86.0	11.20
P-5	91.0	5.80
S-100	63.9	.65
S-101	51.5	.72
S-102	39.2	.86
S-103	32.9	.90
S-104	26.3	1.02
S-105	21.0	1.13
S-106	16.5	1.25
S-107	12.4	1.38
S-108	10.0	1.52
S-110	5.0	1.80
S-112	2.1	2.09
S-201	77.4	.63
S-202	87.5	.64
S-203	105.9	.68
S-204	117.0	.76
S-205	125.2	.86
S-206	132.9	.98
S-207	137.5	1.11
S-208	141.9	1.24
S-209	145.0	1.38
S-210	147.7	1.53
AA	80.0	.10
DD	13.4	1.44
EE	66.5	.76
FF	39.0	.82

[a]Effluent measurements were made aboard the P-2 seacraft at both locations.

TABLE IV.- INSTRUMENT PLAN

Site	Instruments	Effluent measured
P-1	Chemiluminescent detector	HCl
	Bubbler	HCl
	pH paper	HCl
	DIF infrared detector	CO
	Mass monitor	Particles
	Climet light photometer	Particles
	Andersen cascade impactor	Particles
	Nuclepore filter	Particles
P-2	Microcoulometer	HCl
	Chemiluminescent detector	HCl
	Bubbler	HCl
	pH paper	HCl
	DIF infrared detector	CO
	Mass monitor	Particles
	Climet light photometer	Particles
	Andersen cascade impactor	Particles
	Nuclepore filter	Particles
P-3	Bubbler	HCl
	pH paper	HCl
	DIF infrared detector	CO
	Mass monitor	Particles
	Royco light photometer	Particles
	Andersen cascade impactor	Particles
	Nuclepore filter	Particles
P-4	Bubbler	HCl
	pH paper	HCl
	DIF infrared detector	CO
	Mass monitor	Particles
	Andersen cascade impactor	Particles
	Nuclepore filter	Particles
P-5	Bubbler	HCl
	pH paper	HCl
	DIF infrared detector	CO
	Mass monitor	Particles
	Andersen cascade impactor	Particles
	Nuclepore filter	Particles
S-100 to S-210[a]	Bubbler[b]	HCl
	pH paper[b]	HCl
	Nuclepore filter[b]	Particles
DD, EE, FF	Bubbler	HCl
	pH paper	HCl
	Nuclepore filter	Particles
	High volume cascade impactor	Particles
AA	pH paper	HCl
	Nuclepore filter	Particles
	Andersen cascade impactor	Particles

[a]Sites S-100, S-101, S-102, and S-201 were also equipped with mass monitors.

[b]Sites S-100, S-101, and S-201 had two of these instruments.

TABLE V.- INSTRUMENT CAPABILITIES

(a) Gas instruments

Instrument	Species	Detection range	Response time to 90 percent of final reading	Required analysis
Chemiluminescent detector (ref. 12)	HCl	0.05 to 50 ppm	1 to 5 sec	None
Microcoulometer (ref. 13)	HCl	0.1 to 20 ppm	1 to 5 sec	None
Bubbler (ref. 14)	HCl	Greater than 80 ppm-sec	Not applicable	Coulometric
pH paper (ref. 14)	HCl	Qualitative[a]	Not applicable	None
Infrared detector[b]	CO_2	1 to 50 ppm above ambient	2.5 sec	None
DIF infrared detector (ref. 12)	CO	0.5 to 200 ppm	28 sec	None

(b) Particle instruments

Instrument[c]	Particle size range, μm	Detection limit	Response time to 90 percent of final reading	Required analysis
Royco photometer	0.5 to 6.5	1 particle	1 msec	Computer processing
Climet photometer	0.3 to 10.0	1 particle	1 msec	Computer processing
Mass monitor	0.1 to 20.0	10 $\mu g/m^3$	5 sec	None
Nuclepore filter	>0.01	10 μg	Not applicable	Gravimetric NAA
High volume cascade impactor	>0.01	200 μg	Not applicable	Gravimetric NAA
Andersen cascade impactor	0.43 to 11.0	50 μg	Not applicable	Gravimetric NAA
Lundgren cascade impactor	0.5 to 14.0	50 μg	Not applicable	Gravimetric NAA

[a]Detection limit approximately 1 ppm.
[b]Instrument specifications based on manufacturer's data.
[c]Instrument specifications from manufacturer's data or field experience (ref. 14).

TABLE VI.- PARTICLE MEASUREMENTS FOR MANNED SITES

(NUCLEPORE FILTER DATA)

Site	Total mass, μg (a)	Total mass loading, $\mu g/m^3$	Al, μg	Cl, μg	Al mass loading, $\mu g/m^3$
P-1	111	---	1.60	1.36	2.8
P-2	136	35	1.96	2.04	3.6
P-3	144	50	2.04	1.84	3.7
P-4	319	288	30.72	13.32	29.8
P-5	96	---	3.64	2.48	3.9

[a]Includes 116 μg handling effects.

TABLE VII.- HCl MEASUREMENTS FOR UNMANNED SITES

Site	Activation time, T ± min:sec	Total run time, sec	HCl dosage from bubbler,[a] ppm-sec	pH paper color change
S-100	T + 11:33	607	[b]80	No
S-101	T + 11:33	607	[b]80	No
S-102	T + 11:25	608	124	No
S-103	T + 11:25	608	80	No
S-104	T + 11:17	608	80	No
S-105	T + 11:17	608	80	No
S-106	T + 11:17	608	204	No
S-107	T + 11:08	609	80	No
S-108	T + 11:08	609	116	No
S-110	T + 11:00	609	93	No
S-112	T + 11:00	609	80	No
S-201	T + 11:33	607	135	No
S-202	T + 11:25	608	80	No
S-203	T + 11:25	608	80	No
S-204	T + 11:25	608	80	Yes
S-205	T + 11:17	608	80	No
S-206	T + 11:17	608	80	No
S-207	T + 11:17	608	150	No
S-208	T + 11:08	609	101	No
S-209	T + 11:08	609	80	No
S-210	T + 11:00	609	124	No
AA[c]	---------	---	---	Yes
DD	T - 1:00	360	142	No
EE	T - 1:00	360	358	No
FF	T - 1:00	360	216	No

[a]HCl detection limit.
[b]Results for both bubblers located at this site.
[c]Instruments at this site failed to function.

TABLE VIII.- PARTICLE MEASUREMENTS FOR UNMANNED SITES

(NUCLEPORE FILTER DATA)

Site	Total mass, μg (a)	Run time, min	Total mass loading, μg/m^3 (b)	Al, μg	Cl, μg	Al mass loading, μg/m^3
S-100	111	9.8	----	----	-----	-----
S-100	102	9.6	----	2.44	2.56	10.12
S-101	145	9.6	107	3.08	2.56	11.6
S-101	122	9.6	21	2.52	2.04	9.6
S-102	---	----	----	----	-----	-----
S-103	130	10.4	48	2.56	3.12	9.2
S-104	178	9.7	220	2.88	1.76	10.3
S-105	104	11.0	----	1.68	1.96	5.6
S-106	---	----	----	----	-----	-----
S-107	124	9.9	28	2.00	3.76	7.5
S-108	146	9.7	116	2.16	1.88	8.5
S-110	135	9.7	66	5.12	3.36	18.4
S-112	158	9.6	163	----	-----	-----
S-201	123	9.7	24	1.96	1.88	7.2
S-202	151	9.7	125	2.12	2.12	7.7
S-203	119	10.3	9	6.04	2.60	21.5
S-204	155	9.7	149	8.12	2.44	31.5
S-205	185	9.7	248	2.28	19.04	8.3
S-206	295	9.7	709	3.48	2.72	13.8
S-207	175	10.4	197	2.52	1.64	8.5
S-208	87	9.8	----	1.44	1.36	5.4
S-209	468	9.8	1215	1.96	1.60	6.8
S-210	200	7.6	384	1.76	3.04	12.7
AA	---	----	----	----	-----	-----
DD	83	6.0	----	1.68	2.40	5.7
EE	109	6.0	----	2.08	1.96	7.1
FF	86	6.0	----	----	-----	-----

[a]Includes 116 μg handling effects.

[b]Handling effects have been subtracted; average flow of 27.4 liters/min.

TABLE IX.- IN-CLOUD EFFLUENT MEASUREMENT RESULTS

Pass	Elapsed time after launch, min	Altitude, m	Concentration of NO_x, ppb	Concentration of NO, ppb		Concentration of NO_2, ppb		Cloud width, m
				Peak	Average	Peak	Average	
1	5	900	>650	>550	---	>120	---	1000
2	7	1050	600	520	420	100	93	1070
3	14.5	1680	290	220	121	90	63	1800
4	18	1740	(a)	(a)	(a)	(a)	(a)	1000
5	22	1580	105	85	41	25	25	850
6	26	1200	345	260	152	110	65	1440
7	29.5	1200	325	250	145	95	65	1700
8	31	1200	(b)	(b)	(b)	(b)	(b)	(b)
9	34	1050	305	210	134	120	79	1820

[a]Instrument malfunction.
[b]Pass made outside of cloud.

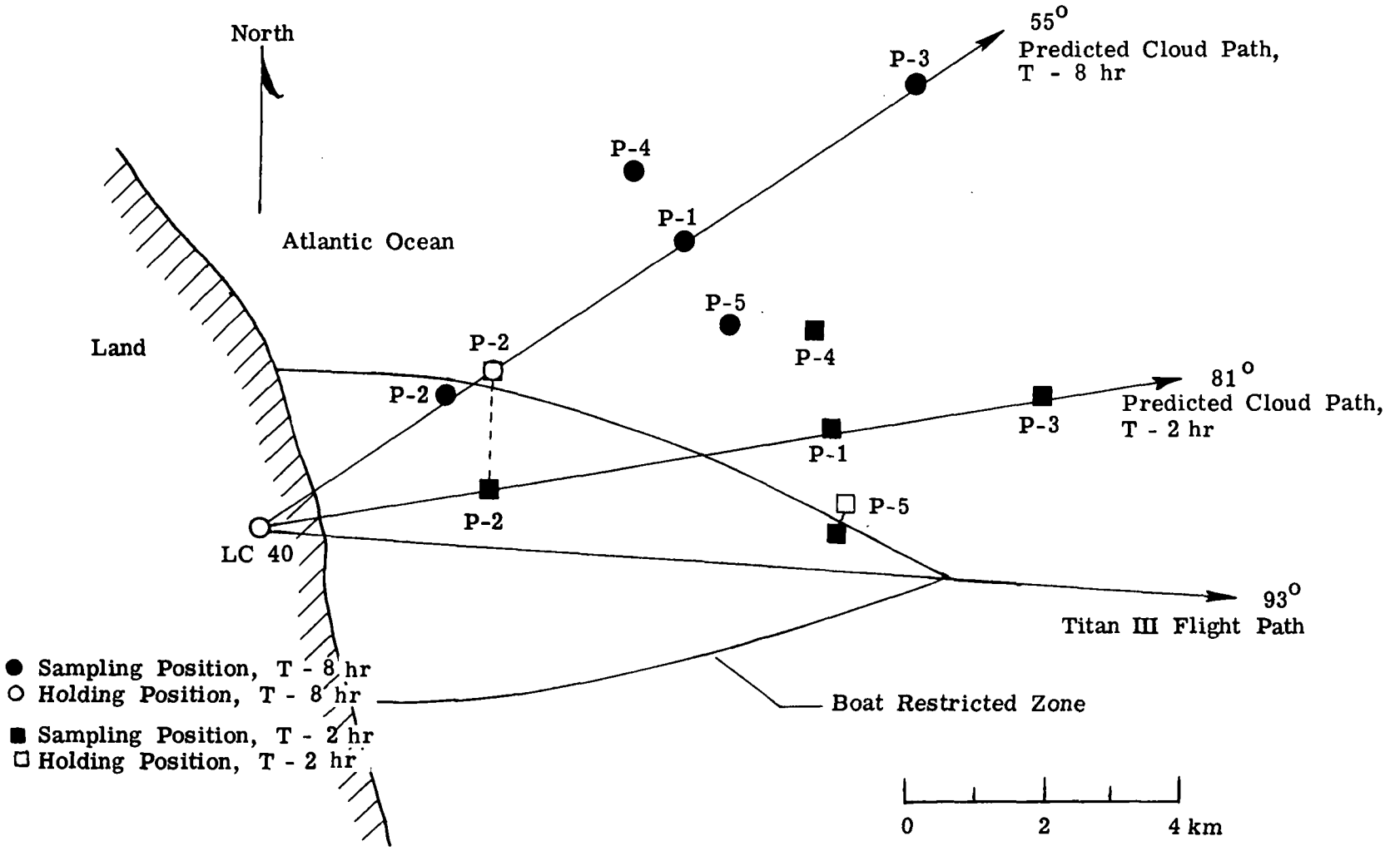

Figure 1.- Nominal seacraft sampling and holding positions based on prelaunch cloud path predictions.

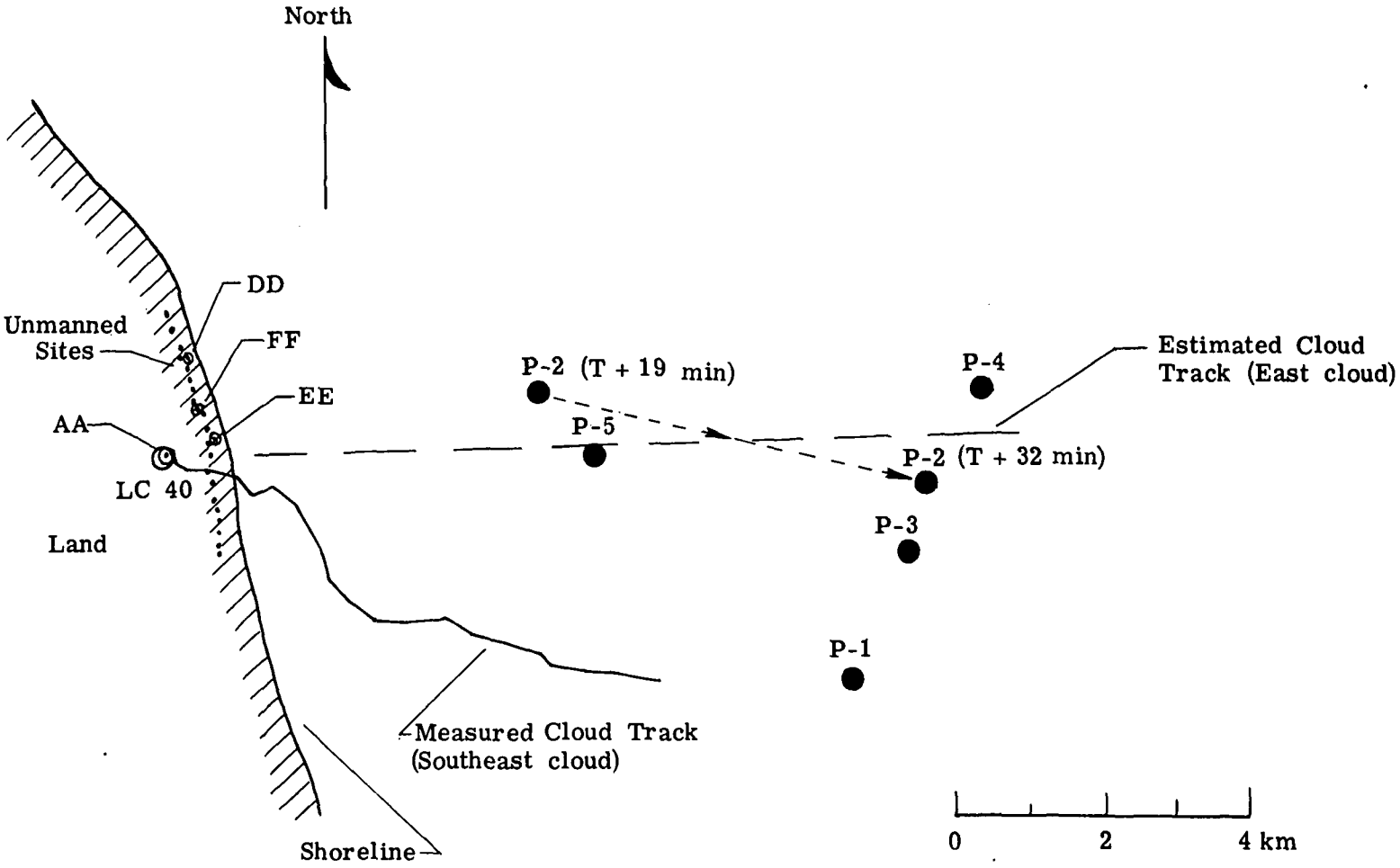

Figure 2.- Final surface effluent sampling locations.

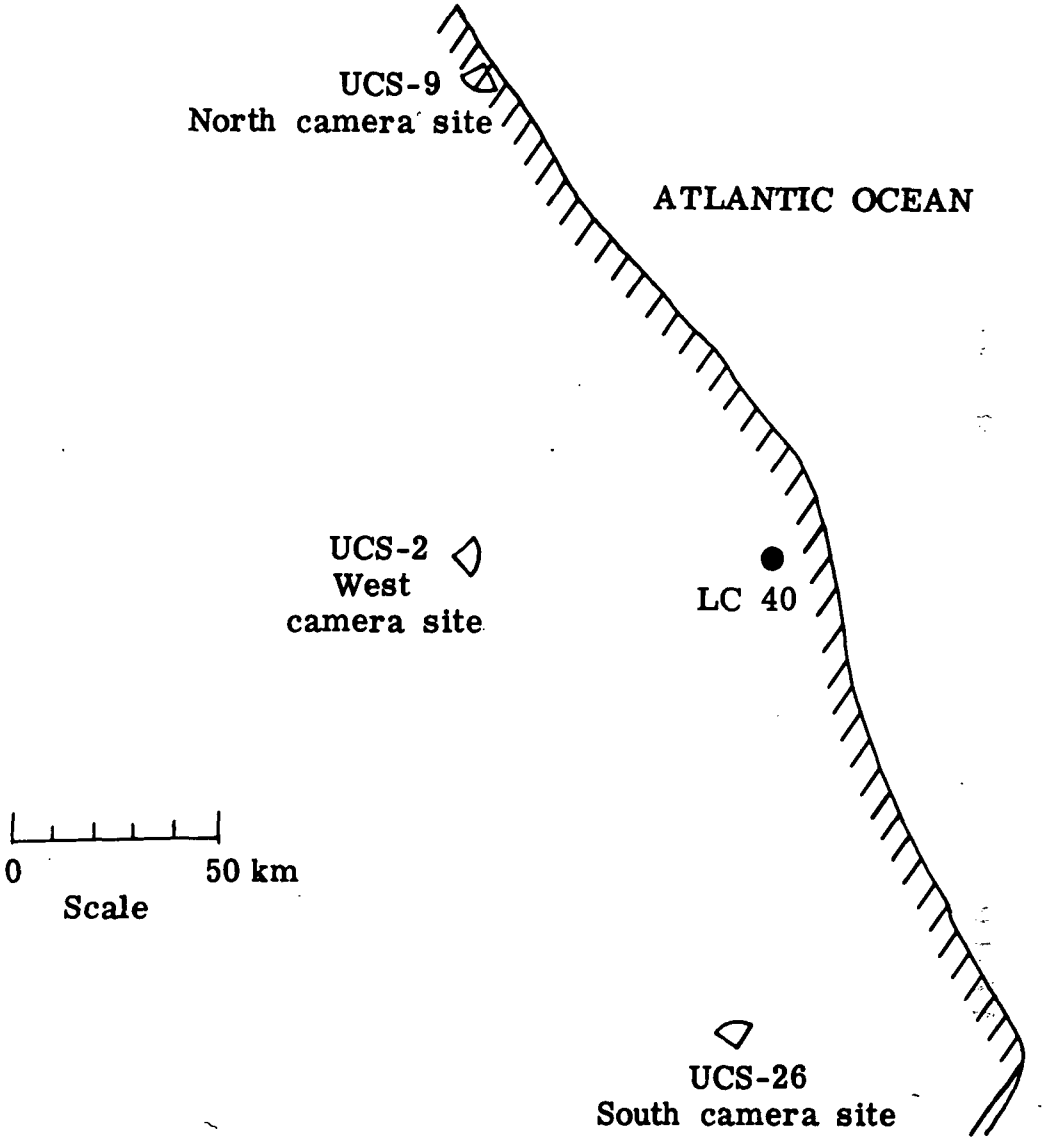

Figure 3.- Camera sites.

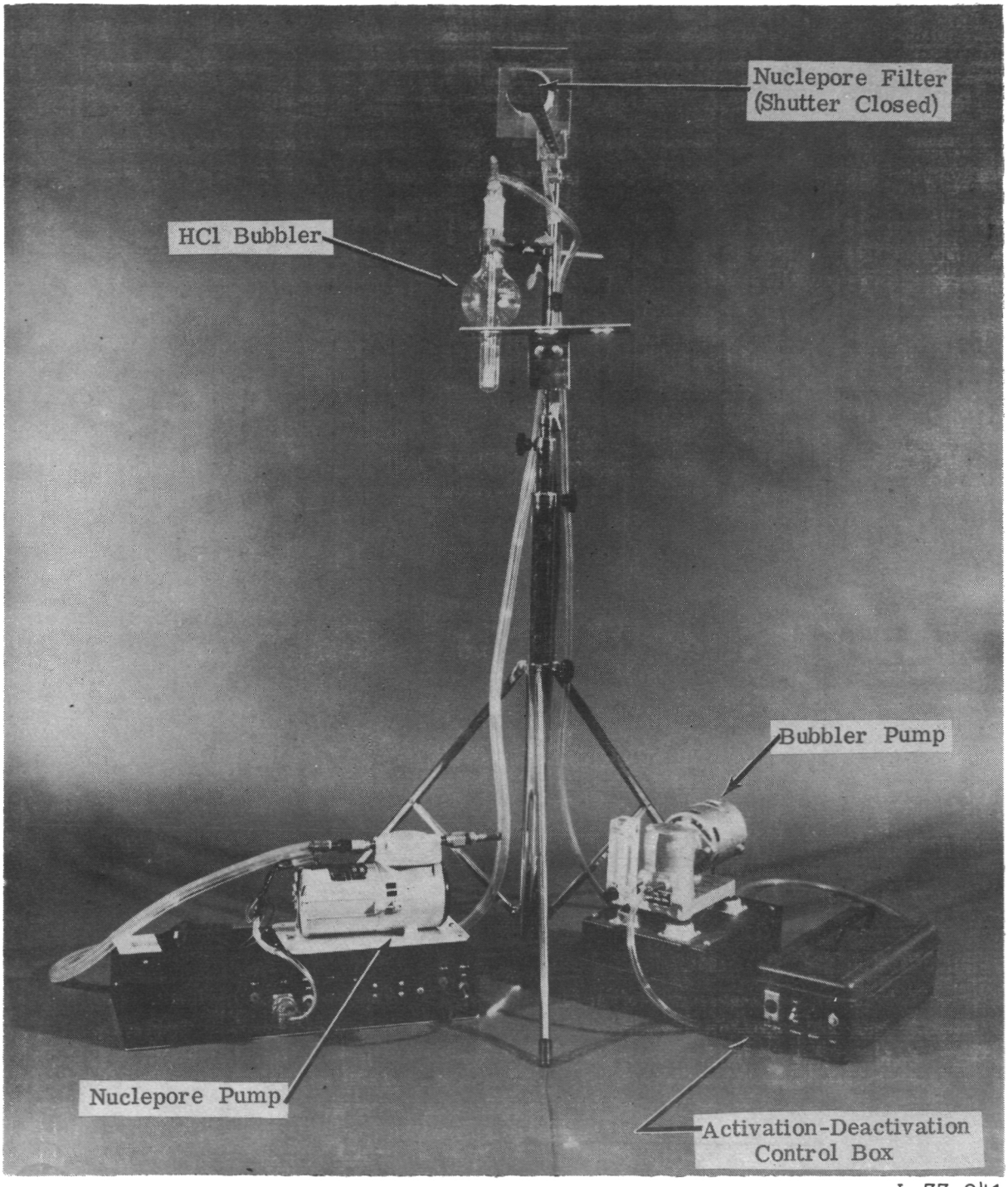

L-77-241

Figure 4.- Typical secondary site.

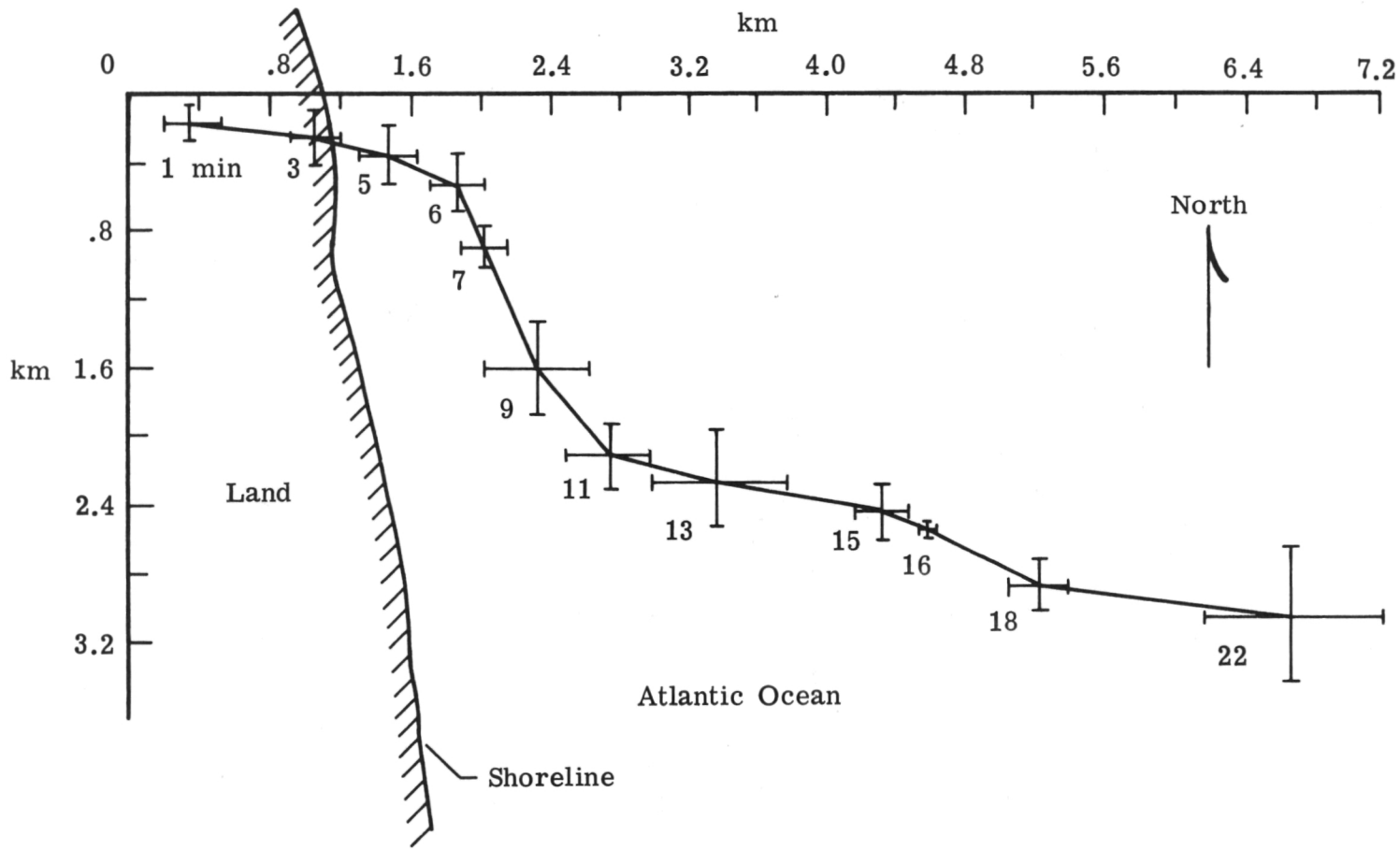

Figure 5.- Ground track of southeast cloud from tracking camera data.

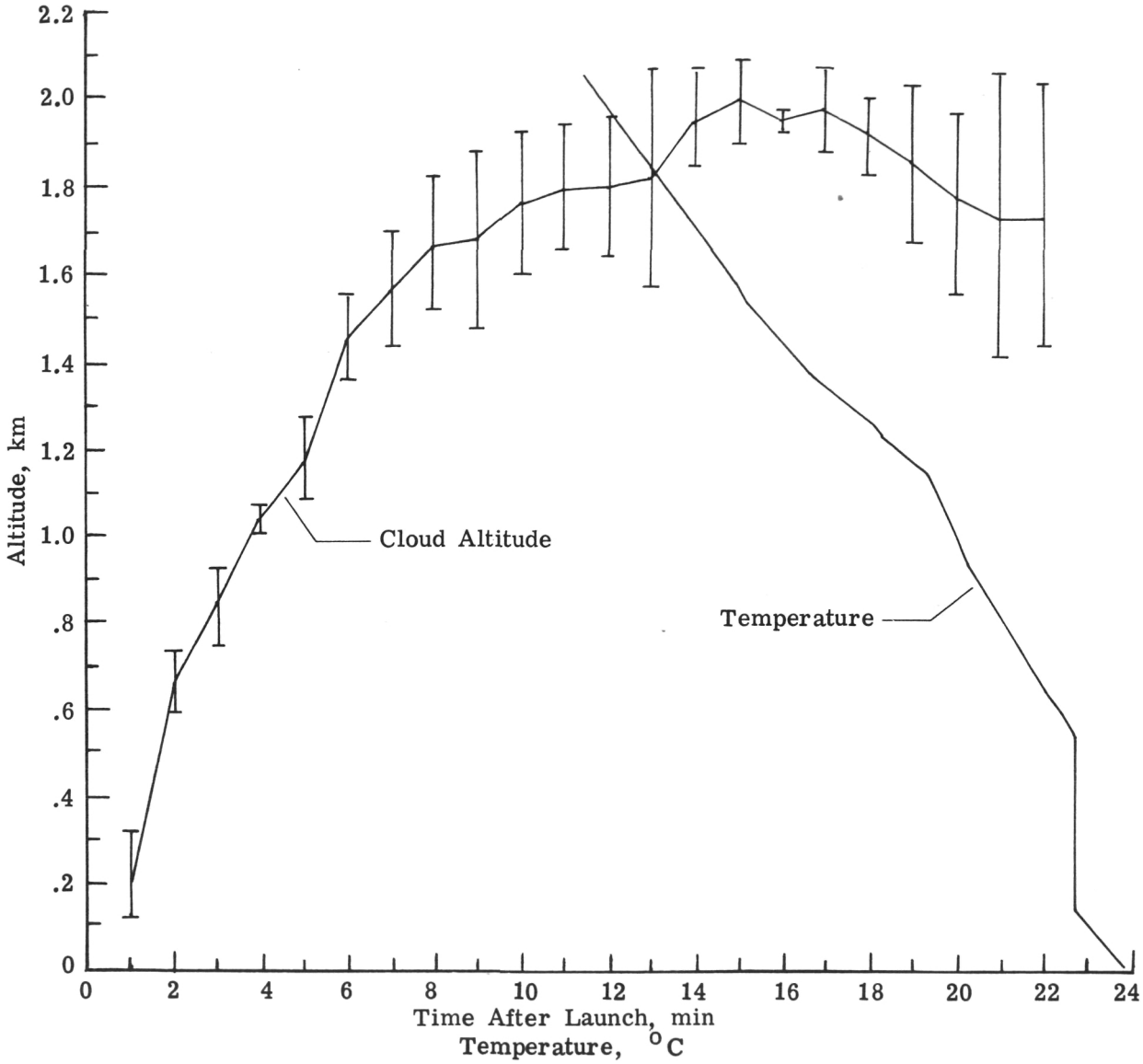

Figure 6.- Cloud altitude from tracking camera data and ambient temperature profile.

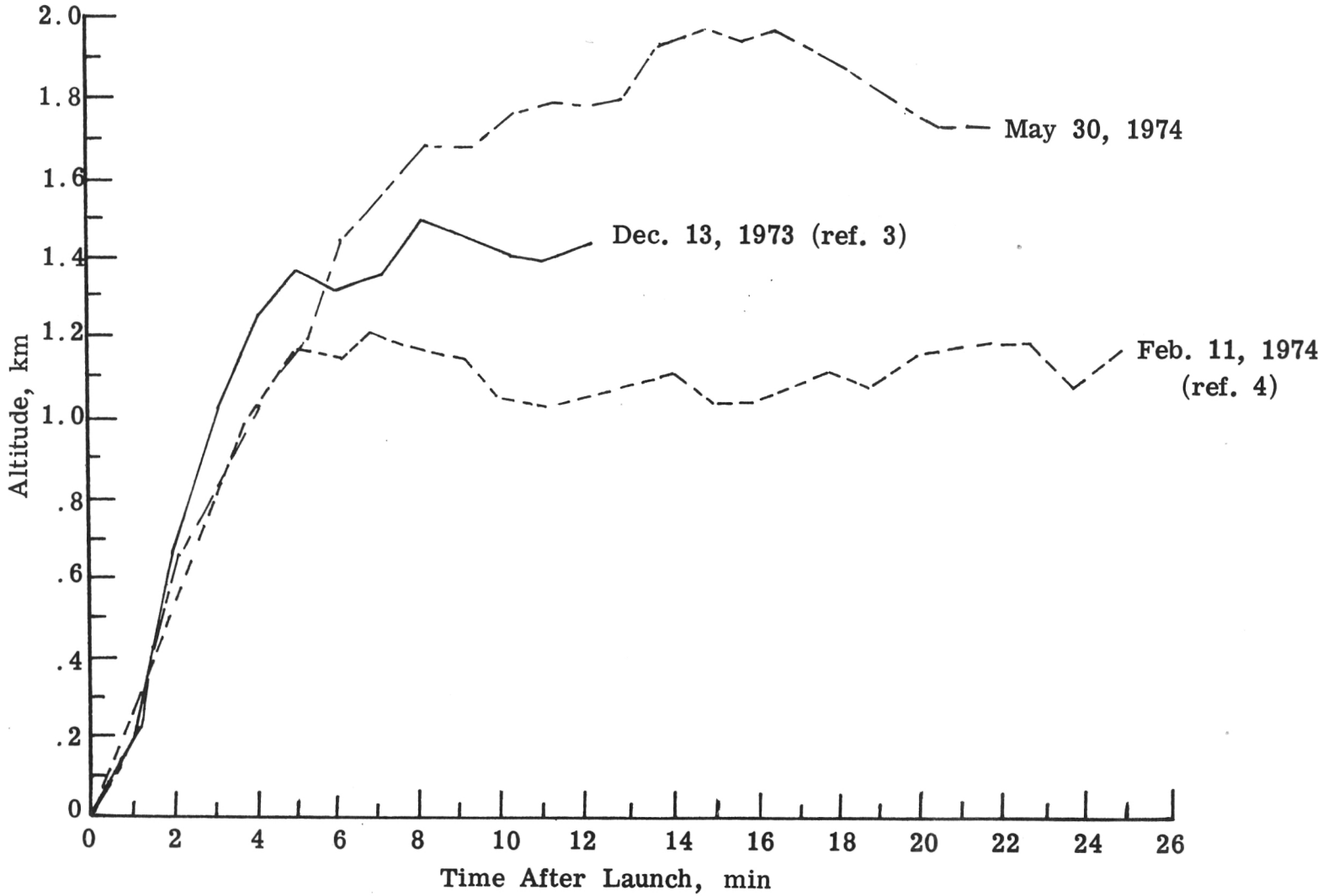

Figure 7.- Cloud altitude measurements for three Titan III ground clouds.

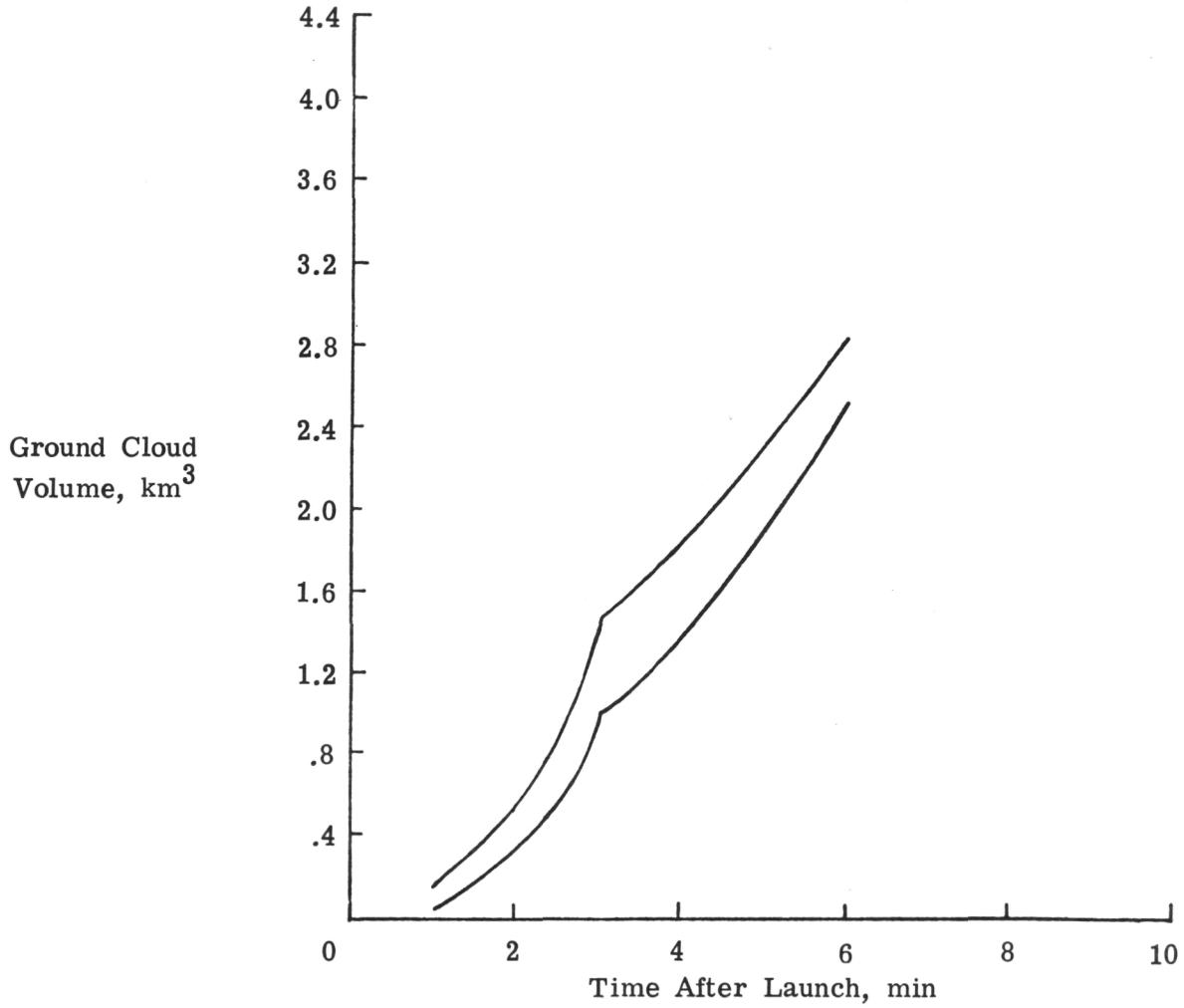

Figure 8.- Time history of ground cloud volume.

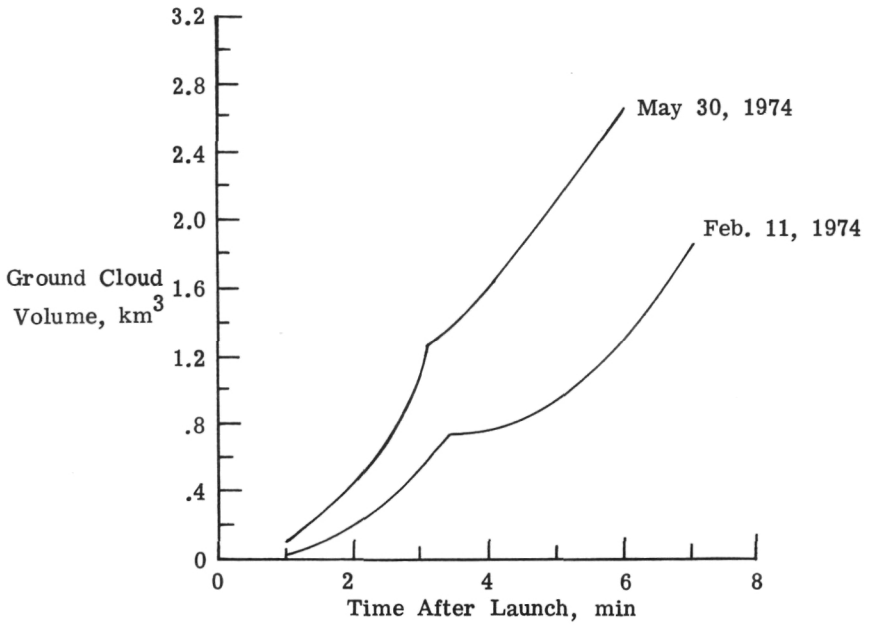

Figure 9.- Comparison of measured ground cloud growth for two Titan III launches.

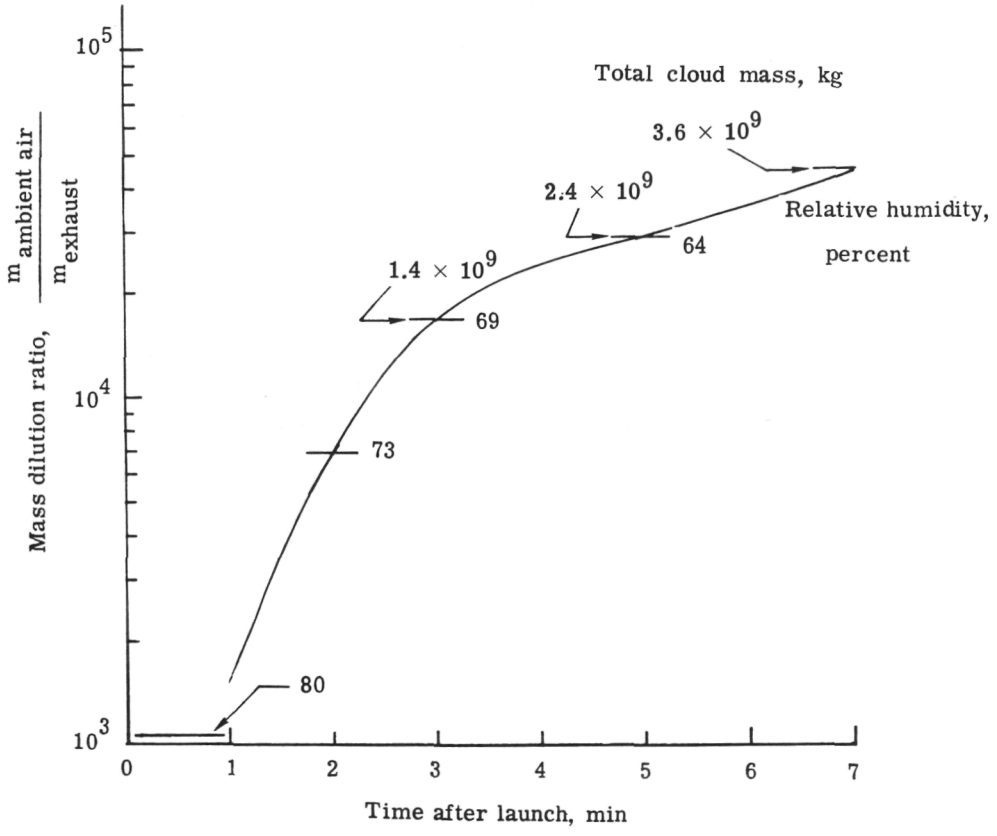

Figure 10.- Ground cloud mass and mass dilution ratio.

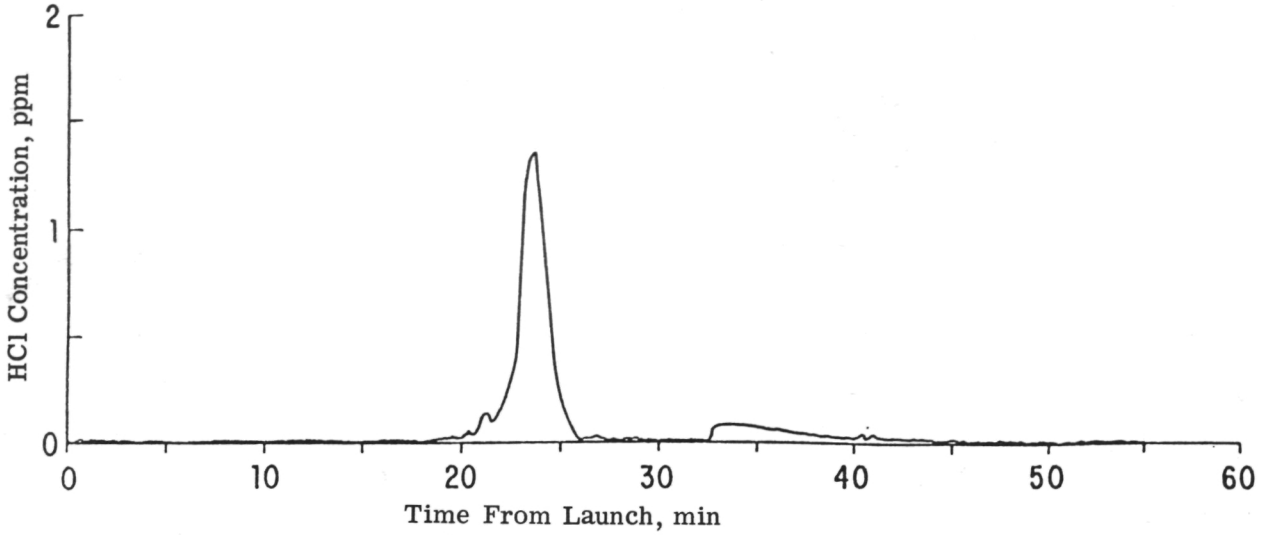

Figure 11.- HCl concentration measured with microcoulometer at site P-2.

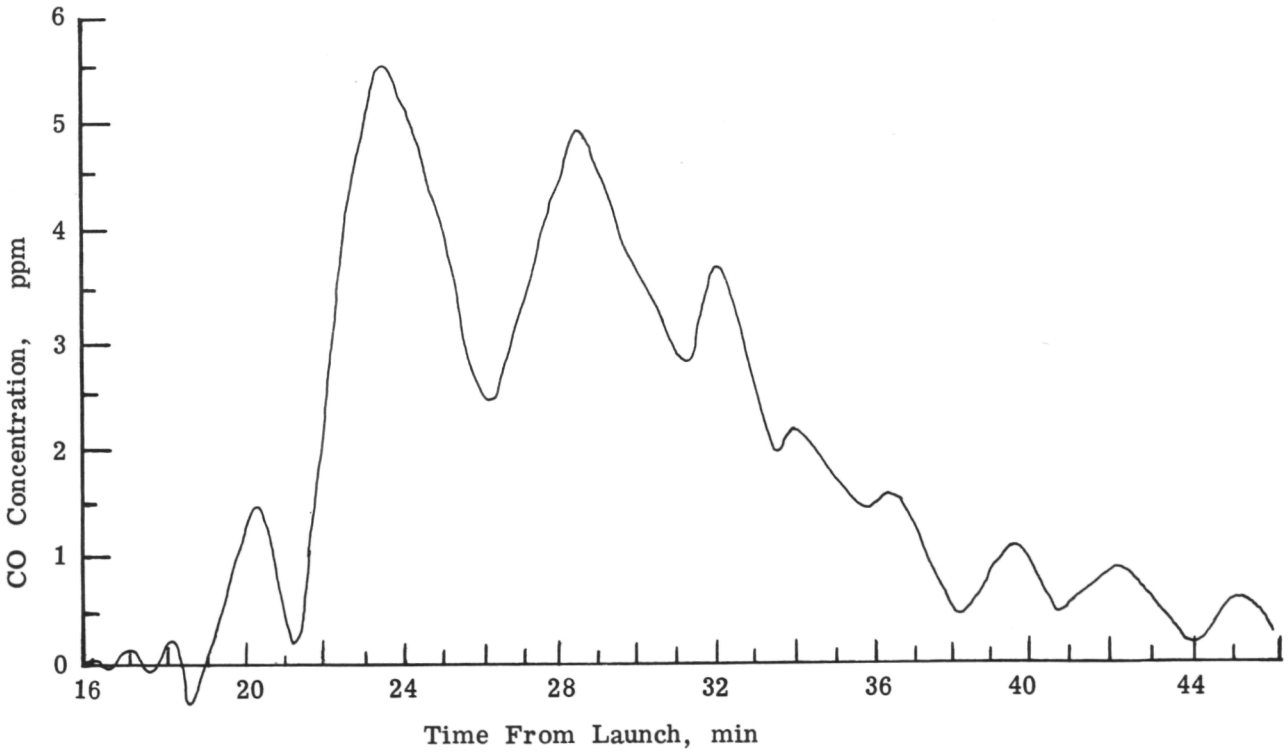

Figure 12.- CO concentration at site P-2.

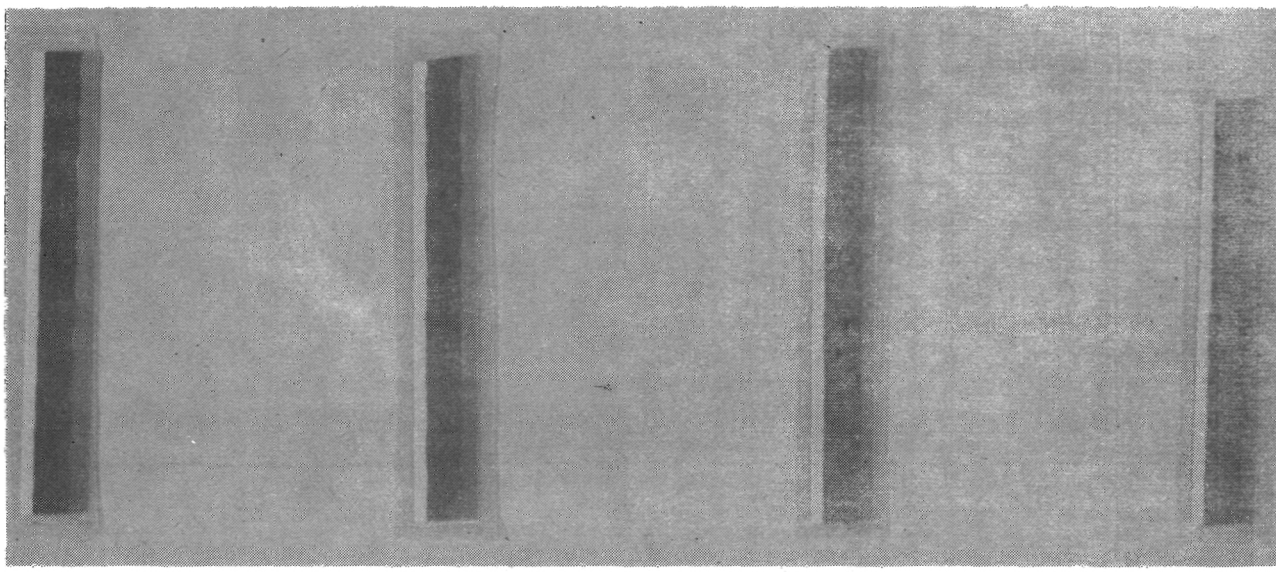

L-77-242

Figure 13.- Spotted pH paper indicating acidic aerosol mist at four measurement sites.

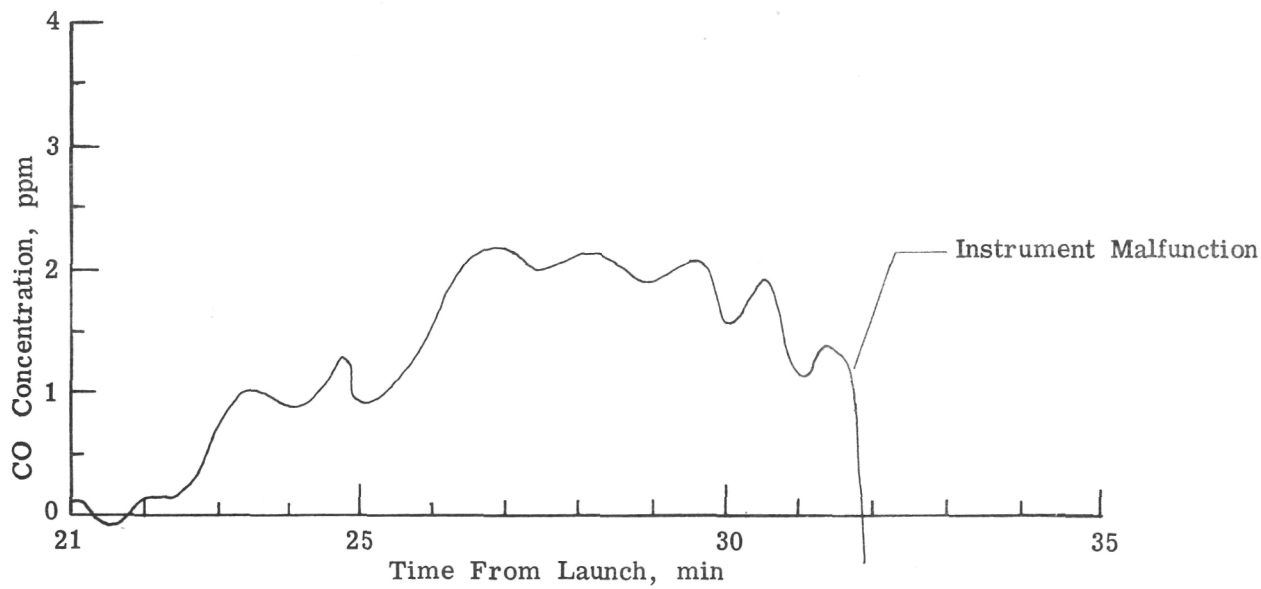

Figure 14.- CO concentration at site P-5.

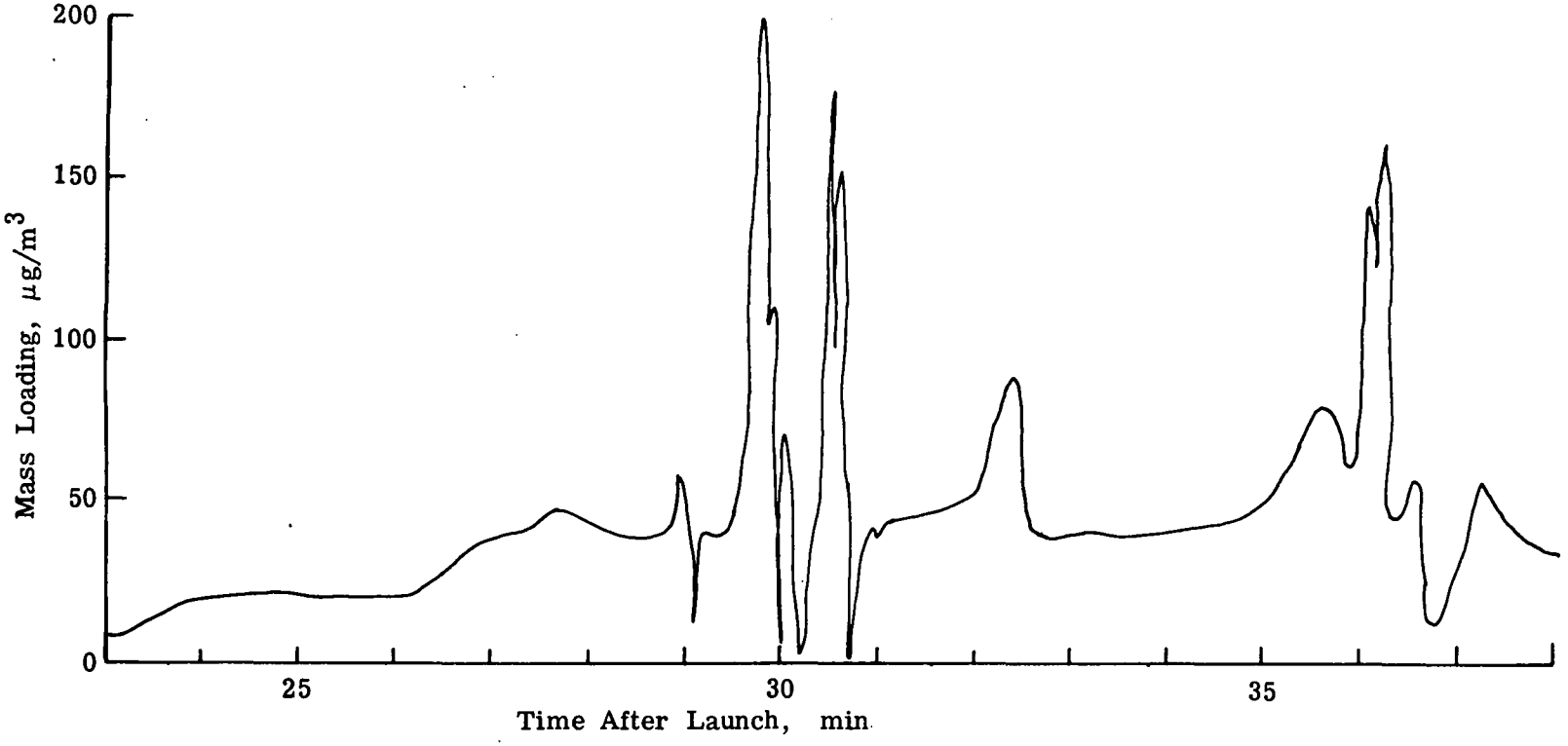

Figure 15.- Particle measurements at site P-5.

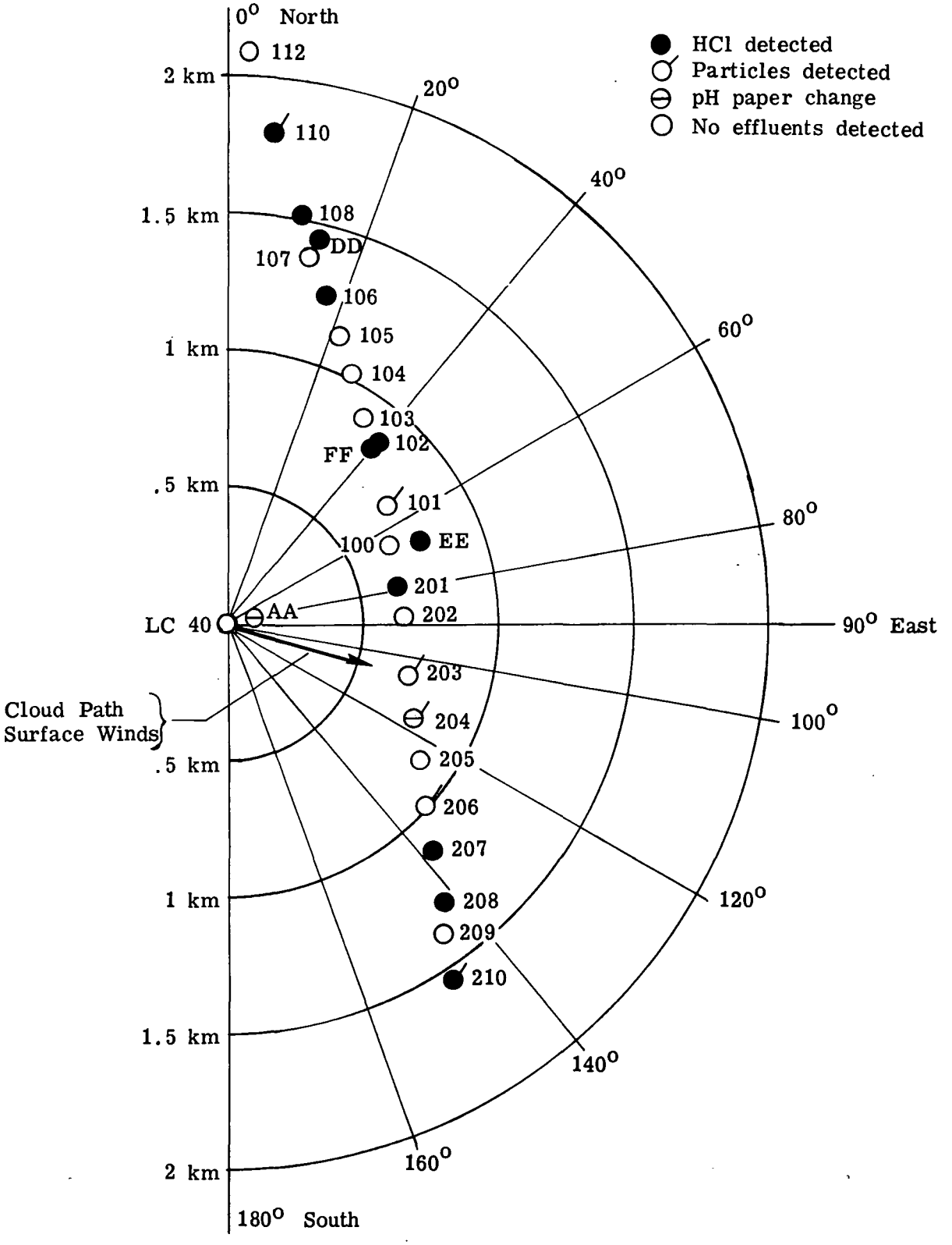

Figure 16.- Effluent measurement results for unmanned sites.

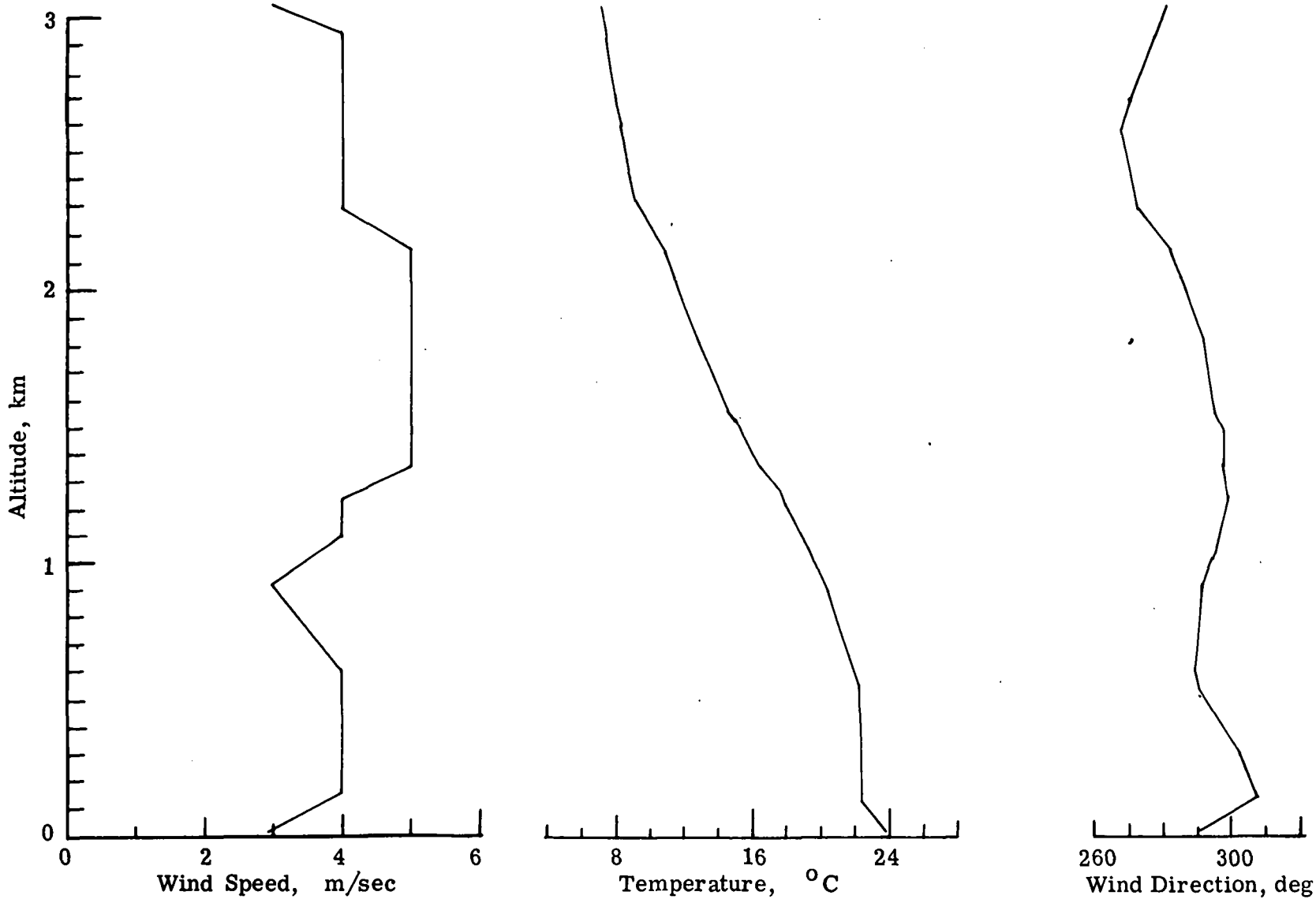

Figure 17.- Measured meteorological conditions at launch time.

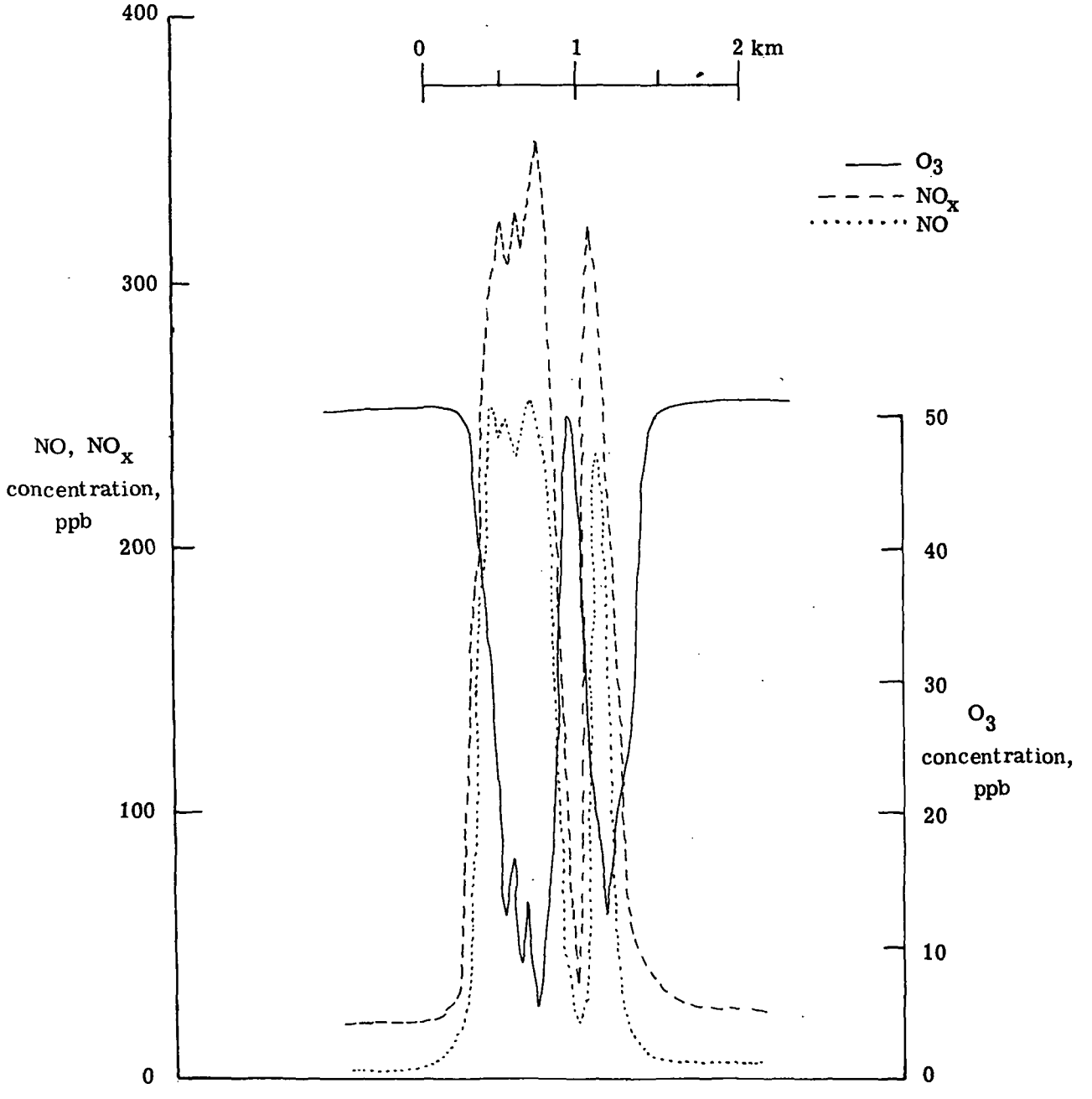

Figure 18.- Typical airborne measurements of NO, NO_x, and O_3 concentrations.

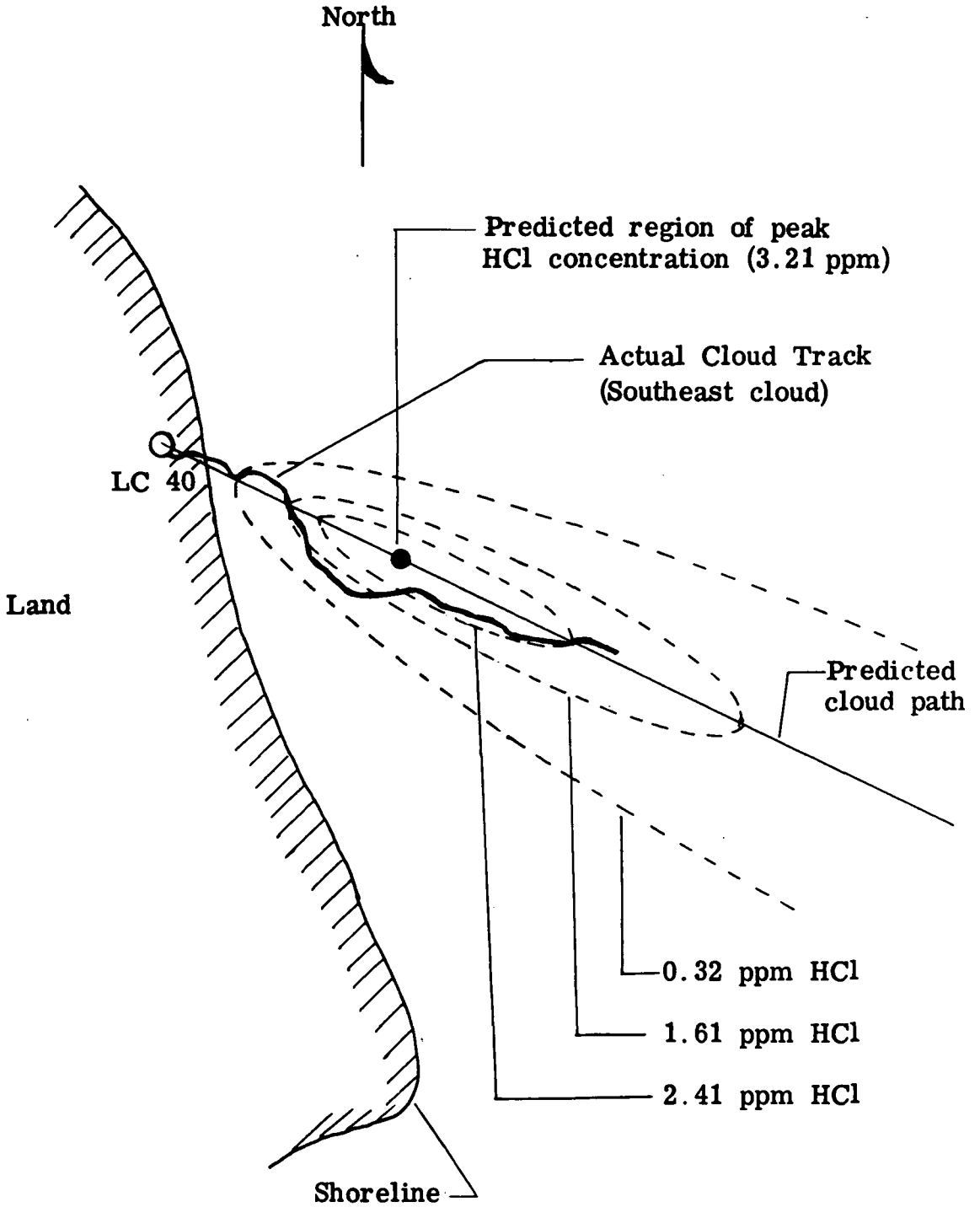

Figure 19.- Postlaunch model predictions of cloud path and HCl concentration compared with measured cloud path.

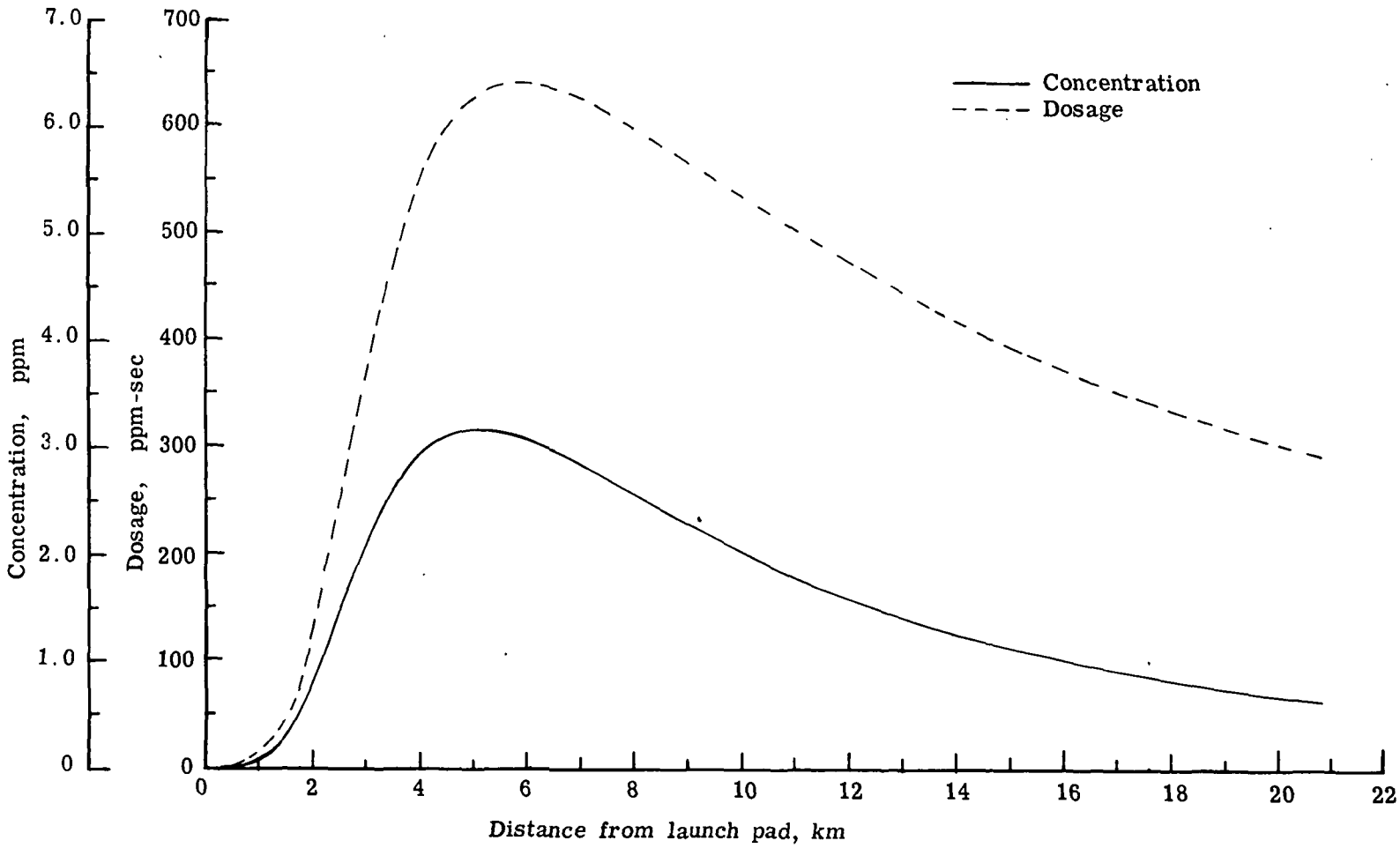

Figure 20.- Postlaunch model predictions of center-line HCl dosage and concentration based on measured meteorological conditions near launch time.

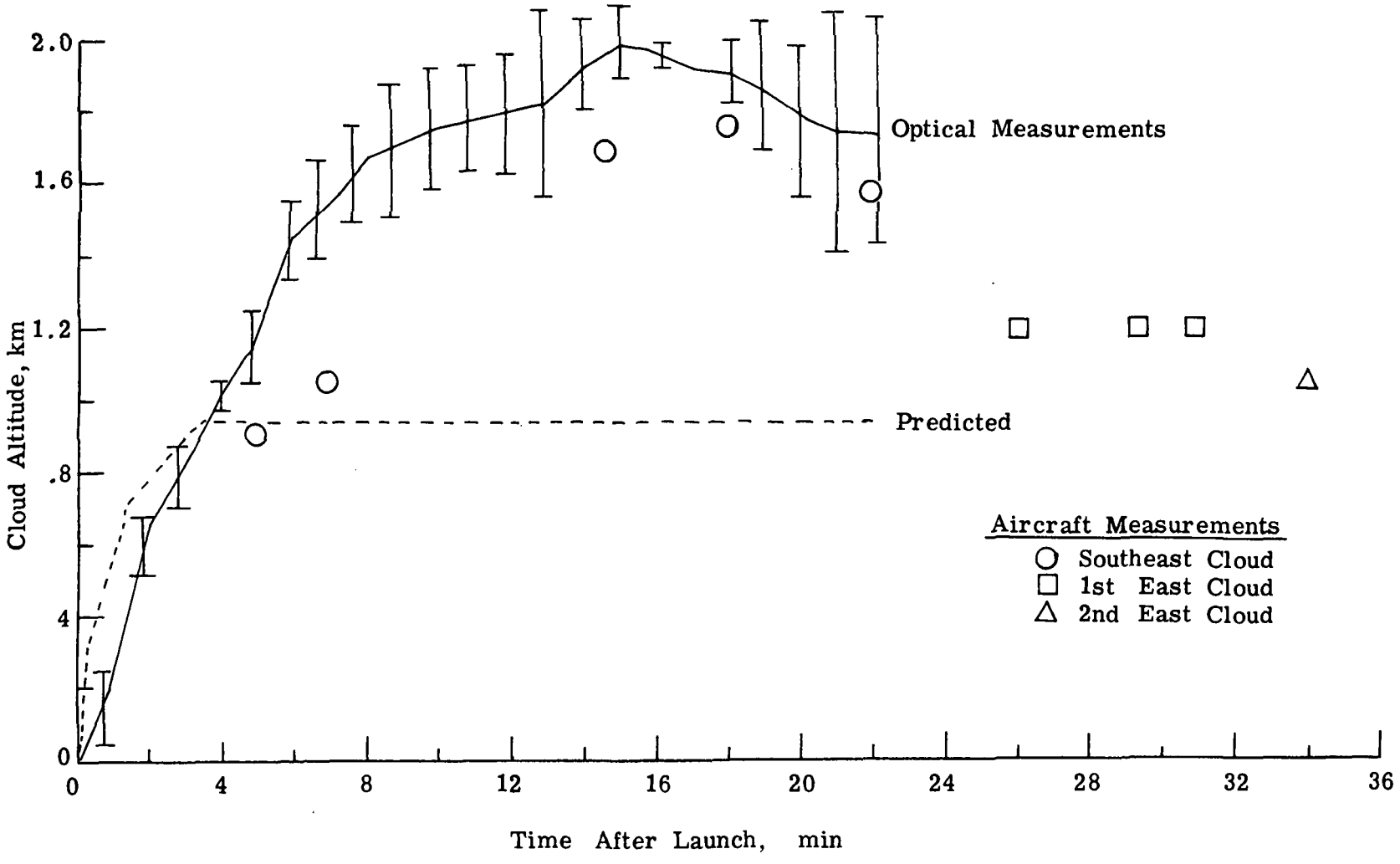

Figure 21.- Postlaunch model prediction of cloud altitude compared with optical and aircraft measurements.

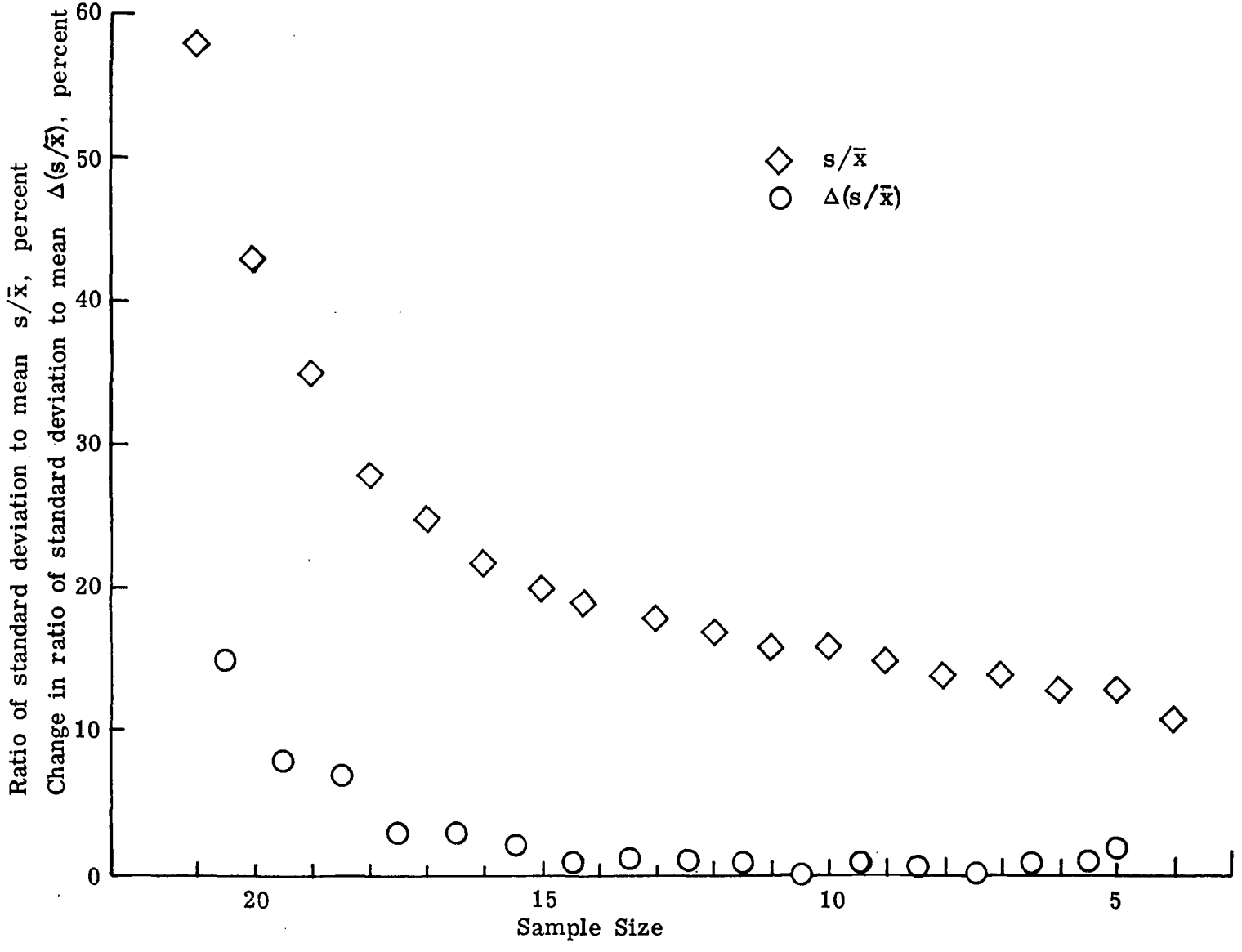

Figure 22.- Statistical treatment of aluminum particulate loading (Nuclepore filter).

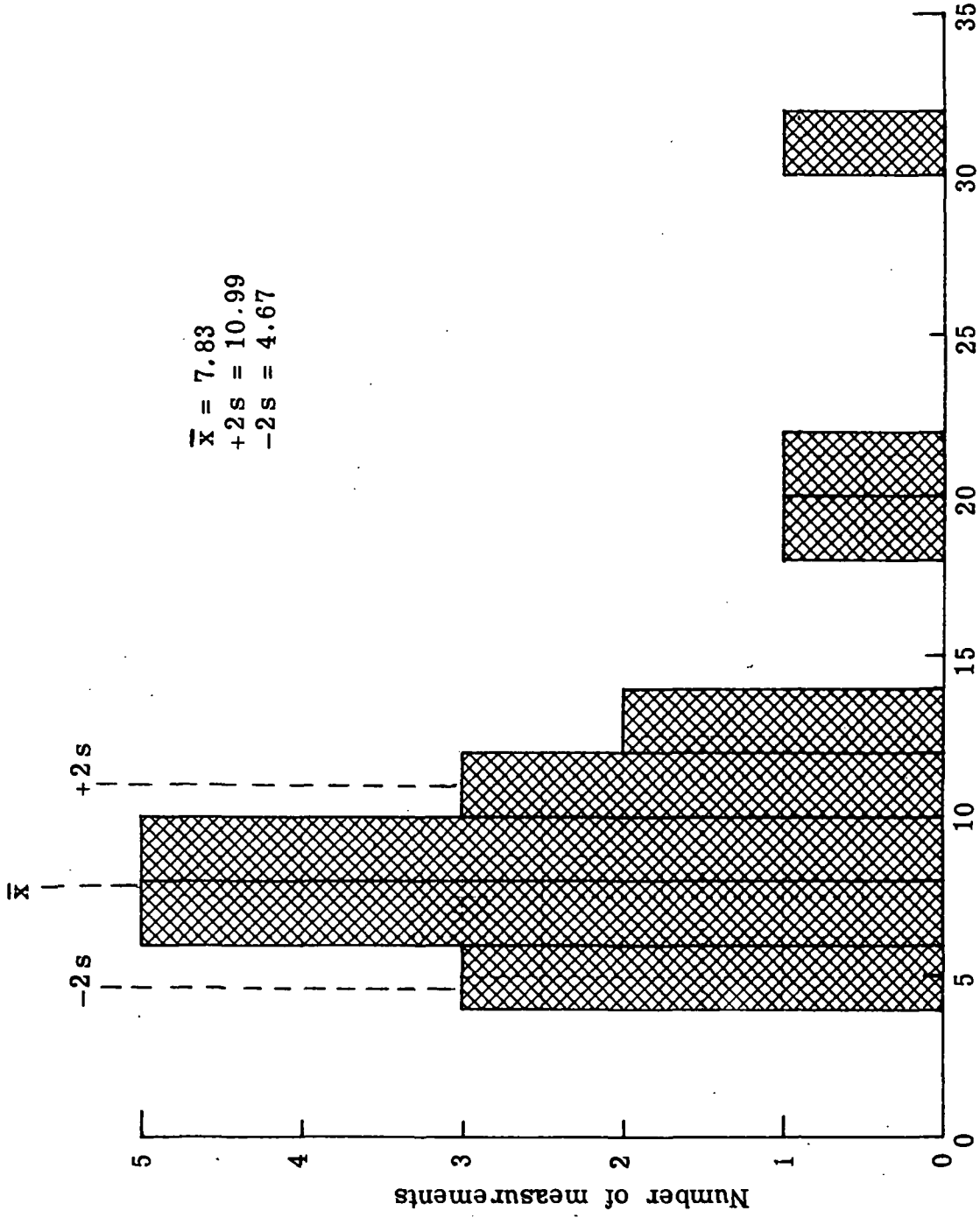

Figure 23.- Distribution of Al mass loading measurements from unmanned sites.

"The aeronautical and space activities of the United States shall be conducted so as to contribute . . . to the expansion of human knowledge of phenomena in the atmosphere and space. The Administration shall provide for the widest practicable and appropriate dissemination of information concerning its activities and the results thereof."

—NATIONAL AERONAUTICS AND SPACE ACT OF 1958

NASA SCIENTIFIC AND TECHNICAL PUBLICATIONS

TECHNICAL REPORTS: Scientific and technical information considered important, complete, and a lasting contribution to existing knowledge.

TECHNICAL NOTES: Information less broad in scope but nevertheless of importance as a contribution to existing knowledge.

TECHNICAL MEMORANDUMS: Information receiving limited distribution because of preliminary data, security classification, or other reasons. Also includes conference proceedings with either limited or unlimited distribution.

CONTRACTOR REPORTS: Scientific and technical information generated under a NASA contract or grant and considered an important contribution to existing knowledge.

TECHNICAL TRANSLATIONS: Information published in a foreign language considered to merit NASA distribution in English.

SPECIAL PUBLICATIONS: Information derived from or of value to NASA activities. Publications include final reports of major projects, monographs, data compilations, handbooks, sourcebooks, and special bibliographies.

TECHNOLOGY UTILIZATION PUBLICATIONS: Information on technology used by NASA that may be of particular interest in commercial and other non-aerospace applications. Publications include Tech Briefs, Technology Utilization Reports and Technology Surveys.

Details on the availability of these publications may be obtained from:

SCIENTIFIC AND TECHNICAL INFORMATION OFFICE

NATIONAL AERONAUTICS AND SPACE ADMINISTRATION

Washington, D.C. 20546